



## P-cadherin regulates human hair growth and cycling via canonical Wnt signaling

Journal:	<i>Journal of Investigative Dermatology</i>
Manuscript ID:	Draft
Manuscript Type:	Original Article
Date Submitted by the Author:	n/a
Complete List of Authors:	Samuelov, Liat; Tel-Aviv Sourasky Medical Center, Dermatology; University of Luebeck, Dermatology Kloepper, Jennifer; University of Luebeck, Dermatology Tsuruta, Daisuke; University of Kurume, Dermatology Bíró, Tamás; University of Debrecen, Physiology Sprecher, Eli; Tel-Aviv Sourasky Medical Center, Dermatology; Sackler Faculty of Medicine, Tel-Aviv University, Human Molecular Genetics & Biochemistry Paus, Ralf; University of Luebeck, Dermatology; University of Manchester, School of Translational Medicine
Key Words:	HJMD, P-cadherin, Hair follicle

**P-cadherin regulates human hair growth and cycling  
via canonical Wnt signaling**

**Liat Samuelov<sup>1,2</sup>, Jennifer E Kloepper<sup>2</sup>, Daisuke Tsuruta<sup>3</sup>, Tamás Bíró<sup>4</sup>, Eli Sprecher<sup>1,5</sup>,  
and Ralf Paus<sup>2,6</sup>**

<sup>1</sup>Department of Dermatology, Tel-Aviv Sourasky Medical Center, Tel-Aviv, Israel

<sup>2</sup>Department of Dermatology, University of Luebeck, Luebeck, Germany

<sup>3</sup>Department of Dermatology, University of Kurume, Kurume, Japan

<sup>4</sup>Department of Physiology, University of Debrecen, Debrecen, Hungary

<sup>5</sup>Department of Human Molecular Genetics & Biochemistry, Sackler Faculty of  
Medicine, Tel-Aviv University, Ramat Aviv, Israel

<sup>6</sup>School of Translational Medicine, University of Manchester, Manchester, UK

**Running title**

P-cadherin regulates human hair growth

**Corresponding author**

Ralf Paus, MD. Dept. of Dermatology, University of Luebeck, Ratzeburger Allee 160, 23538 Luebeck,  
Germany, Tel.: 0451/500-2510 Fax: 0451/500-2981 Email: [ralf.paus@uk-sh.de](mailto:ralf.paus@uk-sh.de)

**The work was conducted at the University of Luebeck, Luebeck, Germany**

## Abstract

P-cadherin is a key component of epithelial adherens junctions, and is prominently expressed in the hair follicle (HF) matrix. Loss-of-function mutations in *CDH3*, which encodes P-cadherin, result in hypotrichosis with juvenile macular dystrophy (*HJMD*), an autosomal recessive disorder featuring sparse and short hair. Here, we attempted to recapitulate some aspects of *HJMD in vitro* by transfecting normal, organ-cultured human scalp HFs with lipofectamine and *CDH3*-specific or scrambled control siRNAs. As in *HJMD* patients, P-cadherin silencing inhibited hair shaft growth, prematurely induced HF regression (catagen) and inhibited hair matrix keratinocyte proliferation. *In situ*, membrane  $\beta$ -catenin expression and transcription of the  $\beta$ -catenin-target gene, *axin2*, were significantly reduced, while GSK3 $\beta$  and phospho- $\beta$ -catenin immunoreactivity were increased. These effects were partially reversed by inhibiting GSK3 $\beta$ . P-cadherin silencing reduced the expression of the anagen-promoting growth factor, IGF-1, while that of TGF $\beta$ 2 (=catagen-promoter) was enhanced. Neutralizing TGF $\beta$  antagonized the catagen-promoting effects of P-cadherin-silencing. In summary, we introduce human HFs as an attractive preclinical model for studying the functions of P-cadherin in human epithelial biology and pathology. This model demonstrate that cadherins can be successfully knocked-down in an intact human organ *in vitro*, and show that P-cadherin is needed for anagen maintenance by regulating canonical Wnt signaling.

Introduction

P-cadherin is a member of the classical cadherin family and a key component of adherens junctions (AJs) in various epithelia, including epidermis and hair follicles (HFs) (Andl *et al.*, 2002; Paredes *et al.*, 2007; Shimoyama *et al.*, 1989). It plays major roles in cell recognition and signaling, morphogenesis and tumor development (Fanelli *et al.*, 2008; Goodwin and Yap, 2004; Paredes *et al.*, 2007). It comprises 5 extracellular domains, a transmembrane domain and a small intracellular domain that interacts with  $\beta$ -catenin. The latter is a crucial player in the canonical Wnt signaling pathway (Fanelli *et al.*, 2008; Heuberger and Birchmeier, 2010; Nelson and Nusse, 2004) (for details, see Figure 1a). Since p63 directly interacts with the promoter for *CDH3*, the gene that encodes P-cadherin, the latter is a p63 target gene (Shimomura *et al.*, 2008).

*CDH3* mutations cause two autosomal recessive disorders, hypotrichosis with juvenile macular dystrophy (*HJMD*; OMIM 601553) and ectodermal dysplasia, ectrodactyly and macular dystrophy (*EEM*; OMIM 225280), which are associated with hair abnormalities. Dermatologically, these patients show sparse and short hair throughout life, an increased percentage of HFs in the regression (catagen) or resting stage (telogen) of the hair cycle and abnormal hair shafts (Supplementary Figure S1a-d) (Bergman *et al.*, 2004; Indelman *et al.*, 2002; Indelman *et al.*, 2007; Jelani *et al.*, 2009; Kjaer *et al.*, 2005; Leibur *et al.*, 2006; Shimomura *et al.*, 2010; Shimomura *et al.*, 2008; Sprecher *et al.*, 2001). While this suggests that P-cadherin is required for normal hair growth, it remains unknown how P-cadherin impacts on the human HF. Unfortunately, P-cadherin deficient mice fail to recapitulate the *HJMD* phenotype (Radice *et al.*, 1997). This suggests that the role of P-cadherin-mediated signaling in human epithelial biology and pathology is best studied directly in human HFs.

To do so, we have generated a novel, widely accessible *in vitro*-surrogate model of HJMD, based on the use of organ-cultured human scalp HFs, a prototypic ectodermal-mesodermal interaction unit (Paus and Cotsarelis, 1999; Schneider *et al.*, 2009). While, evidently, a complex human genetic disorder cannot be expected to be fully recreated *in vitro*, we hoped that such an *in vitro* model could shed new light on how the hair phenotype develops in HJMD patients and on the as yet obscure role of P-cadherin signaling in *human* epithelial biology. Specifically, we asked how P-cadherin silencing in organ-cultured human HFs affects hair growth, cycling and hair shaft formation. In addition, we aimed to obtain indications as to which signaling pathway(s) P-cadherin may use to mediate its HF effects.

## Results

### **P-cadherin expression is strongest in the innermost hair matrix of human anagen hair follicles**

First, we established the protein expression pattern of P-cadherin in fully growing human HFs (i.e., in the anagen VI stage of the hair cycle). Immunohistology showed that, just as in mice (Muller-Rover *et al.*, 1999), P-cadherin protein is most prominently expressed in the innermost cell layer of the human hair matrix (Figure 2a). This confirms the intrafollicular P-cadherin expression pattern previously described by Fujita *et al.*, 1992. However, prominent P-cadherin immunoreactivity (IR) was also seen throughout human epidermis, with sharply reduced expression in its proliferation compartment, i.e. the basal layer of the epidermis (Supplementary Figure S2a). This contrasts with previous reports in both mice and humans that P-cadherin expression is largely confined to the epidermal basal layer (Fujita *et al.*, 1992; Hirai *et al.*, 1989).

**P-cadherin expression declines during catagen**

Since hair cycle-dependent changes in the expression level of molecules during the HF transformation from growth (anagen) to apoptosis-driven HF regression (catagen) frequently indicate a functional role of the molecule under investigation during this organ transformation process (Schneider *et al.*, 2009; Stenn and Paus, 2001), we also examined whether constitutive P-cadherin expression differs between human anagen VI and catagen HFs. Indeed, P-cadherin transcript steady-state levels sharply decline during spontaneous, apoptosis-driven HF regression (catagen) (Figure 2b). This regulated, hair cycle-dependent intrafollicular P-cadherin expression suggests a functional role for P-cadherin during the anagen-catagen transformation, the clinically most important phase in HF cycling (Paus and Foitzik, 2004; Schneider *et al.*, 2009).

**P-cadherin knock-down is possible in human hair follicles and human skin organ culture**

Next, we attempted to silence P-cadherin expression in organ-cultured human anagen scalp HFs (Kloepper *et al.*, 2010) and full-thickness human scalp skin fragments (Lu *et al.*, 2007). P-cadherin gene knock-down was performed by transfection with *CDH3*-specific or scrambled control siRNAs, using lipofectamine. Successful *in situ* knock-down of P-cadherin was documented at the gene and protein level in both, organ-cultured human scalp HFs and epidermis (Figure 2c-f, Supplementary Figure S2b-e). No significant difference in E-cadherin expression was documented following P-cadherin knock-down, indicating the specificity of silencing (Figure S2f-h).

This represents the first successful knock-down of a cadherin family member in an intact human organ and invites exploitation of organ-cultured human HFs and skin as attractive preclinical models for dissecting the molecular and cellular consequences of P-cadherin loss-of-function *in situ*. Availability of such an experimental model constitutes a significant methodological advance, since the functions of P-cadherin-mediated signalling in human epithelial physiology is yet ill-understood (Bandara *et al.*, 2010; Faraldo *et al.*, 2007; Jacobs *et al.*, 2011; Shimomura *et al.*, 2008).

### **P-cadherin silencing results in premature catagen induction and hair growth inhibition**

Since the prominent clinical and histological features of HJMD patients are short and sparse hair since birth, associated with miniaturization and telogen HFs (Supplementary Figure S1a-d), we examined next whether P-cadherin knock-down results in any changes of human hair growth and/or cycling. As assessed by quantitative hair cycle histomorphometry and Ki-67 immunohistomorphometry, this was the case: *in vitro* P-cadherin knock-down prematurely induced catagen development in microdissected, organ-cultured human anagen VI scalp HFs (Figure 2g-l). This was independently confirmed by quantitative Masson-Fontana histochemistry (Kloepper *et al.*, 2010), which revealed the expected sharp reduction in the HF melanin content (data not shown) as a result of the catagen-associated switch-off of intrafollicular melanogenesis (Slominski *et al.*, 2005). Furthermore, P-cadherin silencing *in vitro* resulted in significant inhibition of hair shaft growth (Figure 3).

Therefore, P-cadherin-knock-down in healthy human scalp HFs *in vitro* partially recapitulates the hair growth inhibition that is seen in HJMD patients with mutated

*CDH3 in vivo* (Sprecher *et al.*, 2001). That was associated with a significant inhibition of hair matrix keratinocyte proliferation in catagen and anagen HFs (see Figure 2k-l), which explains the reduced rate of hair shaft formation and is in line with the observed premature catagen development in P-cadherin-silenced human HFs.

**Ultrastructurally, P-cadherin silencing causes hair follicle dystrophy**

The hair growth-inhibitory effect of P-cadherin silencing *in situ* was followed-up on the ultrastructural level. Transmission electron microscopy showed that, compared to scrambled-control treated HFs, P-cadherin-silenced HFs contain large, abnormal aggregates of keratin clumps inside the cytoplasm of precortical hair matrix keratinocytes (Supplementary Figure S3a-b), while no ultrastructural abnormalities were detected in the hair shaft cortex and medulla, except for narrower intercellular spaces (Supplementary Figure S3c-f).

Quantitative TUNEL immunohistomorphometry showed that the number of apoptotic keratinocytes in the precortical hair matrix is not significantly higher than in control HFs treated with scrambled oligos (data not shown). Therefore the observed keratin clumping phenomenon suggests a defect in the correct intracellular transport and arrangement of keratin filaments in the absence of adequate P-cadherin levels/signaling, and is unlikely to result indirectly from enhanced, catagen-associated hair matrix keratinocyte apoptosis. The concept of a defect in keratin transport and arrangement is also in line with the observed HF dystrophy and reduced hair shaft formation.



### P-cadherin silencing impairs normal hair keratin expression

In order to obtain additional pointers to how P-cadherin silencing may impair hair shaft formation and may cause HF dystrophy, gene expression profiling was performed. Microarray analysis and confirmatory Q-PCR analyses revealed that three different hair keratins (KRT36, KRT37 and KRT84) are significantly upregulated by P-cadherin silencing (Supplementary Figure S4a-c). Although this remains to be functionally tested, this abnormal hair keratin expression profile may relate to the observed hair shaft inhibition *in vitro* (Figure 3) and/or to the abnormal hair phenotype seen in HJMD patients *in vivo* (Supplementary Figure S1a-b) (Bergman *et al.*, 2004; Sprecher *et al.*, 2001).

### P-cadherin silencing affects the expression of prominent hair cycle regulators

Subsequently, we wished to explore whether the P-cadherin silencing-induced hair cycle abnormality goes along with changes in two key hair cycle-regulatory growth factors, i.e. insulin-like growth factor 1 (IGF-1) and transforming growth factor beta 2 (TGF $\beta$ 2) (Hibino and Nishiyama, 2004; Philpott *et al.*, 1994; Schneider *et al.*, 2009; Soma *et al.*, 2002; Stenn and Paus, 2001; Weger and Schlake, 2005). The steady-state mRNA level of IGF-1, the key growth factor that maintains HFs in anagen (Ben Amitai *et al.*, 2006; Kwack *et al.*, 2009; Philpott *et al.*, 1994; Zhao *et al.*, 2011), significantly declines after P-cadherin knock-down (Figure 4a).

In contrast, the IR of TGF $\beta$ 2, the key catagen-inducing growth factor (Hibino and Nishiyama, 2004), significantly increases in P-cadherin-silenced HFs (Figure 4b-d). This is functionally important, since the effects of P-cadherin knock-down on HF growth and cycling can be partially reversed by culturing P-cadherin-silenced HFs in the presence of TGF $\beta$ -neutralizing antibody (Supplementary Figure S5a-d). Thus, P-

cadherin-mediated signaling may be required to maintain human HFs in anagen, at least in part, via suppressing TGF $\beta$ 2 expression and by maintaining sufficient IGF-1 levels.

**P-cadherin silencing regulates canonical Wnt signaling**

P-cadherin and the Wnt signaling pathway rely on the same pool of cytoplasmic  $\beta$ -catenin (Gottardi and Gumbiner, 2001; Heuberger and Birchmeier, 2010; Kuphal and Behrens, 2006) (Figure 1a), and adequate Wnt signaling is thought to be important for anagen maintenance in murine HFs (Li *et al.*, 2011; Schneider *et al.*, 2009; Shimizu and Morgan, 2004; Van Mater *et al.*, 2003). Therefore, we finally investigated whether P-cadherin silencing affects  $\beta$ -catenin stabilization and Wnt target gene expression in human keratinocytes of the innermost hair matrix, i.e. the site of maximal intrafollicular P-cadherin expression (see Figure 2a). To this end,  $\beta$ -catenin and glycogen synthase kinase 3 beta (GSK3 $\beta$ ) expression was assessed immunohistologically.

After intrafollicular P-cadherin silencing membrane  $\beta$ -catenin IR is significantly reduced, while GSK3 $\beta$  and phospho- $\beta$ -catenin protein expression is significantly increased *in situ* (Figure 5a-g). Therefore, P-cadherin silencing in keratinocytes of the innermost hair marix significantly likely upregulates  $\beta$ -catenin degradation through GSK3 $\beta$ . This is expected to result in reduced active  $\beta$ -catenin available for the Wnt signaling pathway (Figure 1b). Further evidence of reduced  $\beta$ -catenin activity by P-cadherin knock-down was obtained by demonstrating that transcription of a key  $\beta$ -catenin target gene, axin 2 (Lovatt and Bijlmakers, 2010), is reduced in silenced HFs (Figure 5h). These effects (i.e. axin2 downregulation and phospho- $\beta$ -catenin upregulation following P-cadherin knock-down) are partially reversed by culturing P-

cadherin-silenced HFs in the presence of the potent GSK3 $\beta$  inhibitor, lithium chloride (LiCl) (Tighe *et al.*, 2007) (Figure 5i-k).

Taken together, these experiments demonstrate P-cadherin to be a key regulator of canonical Wnt signaling in human HFs, whose maintenance appears to be critical for sustaining HFs in their growth phase (anagen).

## Discussion

Here we provide the first evidence that P-cadherin protein expression and its presence in adherens junctions is essential for normal epithelial growth in an intact human organ. Specifically, we document that P-cadherin operates as a potent, novel regulator of human hair shaft formation and hair growth – the first time that a member of the cadherin family is directly shown to play an essential regulatory role in the control of normal human HF growth and cycling.

Our data suggest that P-cadherin maintains human HFs in anagen through activation of canonical Wnt signaling and operates as a major molecular brake on HF regression (catagen) by inhibiting GSK3 $\beta$ -mediated  $\beta$ -catenin degradation, thereby ensuring active canonical Wnt signaling (Figure 1a). This is well in line with the increasing recognition that canonical Wnt signaling is crucial for murine hair growth (Andl *et al.*, 2002; Baker *et al.*, 2010; Huelsken *et al.*, 2001; Li *et al.*, 2011; Millar, 2002; Schneider *et al.*, 2009; Shimizu and Morgan, 2004; Van Mater *et al.*, 2003). This concept is supported by our findings that P-cadherin maintains expression of the anagen-promoting growth factor, IGF-1, while it suppresses the chief catagen-promoting growth factor, TGF $\beta$ 2.

The current experiments suggest that, if normal P-cadherin-mediated signaling is

antagonized by gene silencing, or becomes dysfunctional due to *CDH3* gene mutations (HJMD), this results in a decrease of membrane-bound  $\beta$ -catenin. The latter likely is released from the cadherin-catenin complex in hair matrix keratinocytes and is targeted for ubiquitination and degradation, as attested by the observed upregulation of GSK3 $\beta$  and phospho- $\beta$ -catenin after P-cadherin silencing. This, in turn, is expected to sharply reduce the amount of cytoplasmic  $\beta$ -catenin available for canonical Wnt signaling, thus resulting in the downregulation of key  $\beta$ -catenin target genes required for anagen maintenance (for details, see Figure 1b) (Andl *et al.*, 2002; Baker *et al.*, 2010; Huelsken *et al.*, 2001; Schneider *et al.*, 2009).

The observed keratin clumping may result from defective intracellular transport and arrangement of keratin filaments in the absence of adequate P-cadherin levels/signaling. This fits well to the observed HF dystrophy and reduced hair shaft formation, and is in line with the concept that P-cadherin is a direct p63 target gene (Shimomura *et al.*, 2008), since p63 constitutes a crucial control of normal keratinization (Kim *et al.*, 2009; Mikkola *et al.*, 2010). Perhaps, this p63 connection also explains the abnormal hair keratin gene expression after P-cadherin silencing (Supplementary Figure S4a-c).

Just as in murine HFs (Muller-Rover *et al.*, 1998), P-cadherin is the only classical cadherin that is physiologically expressed in the innermost hair matrix, i.e. at the interface with the inductive HF mesenchyme (Figure 2a, Supplementary Figure S2g-h). Therefore, it is conceivable that this special epithelial HF compartment depends on adequate P-cadherin signaling for normal epithelial cell function and anagen maintenance. This may render hair matrix keratinocyte proliferation, terminal keratinocyte differentiation in the precortical hair matrix, and consequently hair shaft formation from this cell pool very sensitive to P-cadherin silencing and P-cadherin genetic dysfunction.

Moreover, our data suggest that the innermost cell layer of the matrix has the capacity to regulate the human hair cycle *independently* from epithelial stem cells in the – much more distally located - HF bulge (which is absent under the current HF organ culture conditions). Therefore, this region of the hair matrix must generate as yet unknown, P-cadherin-dependent signals that impact on whether a HF stays in anagen or enters into catagen and, which translate into changes in the intrafollicular balance between anagen-maintaining and catagen-promoting growth factors (e.g. IGF-1 versus TGF $\beta$ 2). To elucidate these P-cadherin-dependent signals that impact on and/or emanate from the innermost hair matrix, certainly is an important future research target.

The effects of P-cadherin silencing in normal adult human scalp HFs *in vitro* correspond well to the hair phenotype of patients with HJMD and EEM syndromes, who characteristically exhibit an abnormally high percentage of catagen HFs and reduced hair shaft formation (Bergman *et al.*, 2004; Sprecher *et al.*, 2001). Therefore, our study also provides a novel, clinically relevant *surrogate model* for studying *in vitro* a) the general consequences of P-cadherin loss-of-function in human epithelial biology *in situ*, and b) the pathomechanisms that underlie the complex and as yet ill-understood hair phenotype seen in HJMD and EEM patients.

## Materials and Methods

### Tissue collection

Human anagen VI HFs were isolated from scalp skin obtained from six patients undergoing routine face-lift surgery (one man and five women aged 42-59 years; mean age 50 years) after informed consent and institutional ethics committee approval.

**P-cadherin knock-down**

In four HF cultures, HFs were transfected once with human P-cadherin siRNA (Sigma-Aldrich, Munich, Germany, SASI\_Hs02\_00332561, 5'-CCAAUAUCUGUCCCUGAAA-3') at day 0, while in two additional cultures HFs were transfected twice , i.e. at days 0 and 3. HFs treated with control siRNA (scrambled oligos; Santa Cruz, CA, USA, sc-37007) served as control. After transfection (and between the two transfections in the two additional cultures mentioned above) HFs were maintained in a 24-well plate with 500µl William's E medium (Biochrom, Cambridge, UK) supplemented with 1% L-glutamine (Invitrogen, Paisley, UK), 0.02% hydrocortisone (Sigma-Aldrich), 0.1% insulin (Sigma-Aldrich) and 1% antibiotic/antimycotic mixture (Gibco, Karlsruhe, Germany) (Philpott *et al.*, 1990). All reagents required for transfection were obtained from Santa Cruz Biotechnology Inc (siRNA transfection reagent, sc-29528; siRNA transfection medium, sc-36868). HF transfection was performed according to the manufacturer's protocol (Santa Cruz Biotechnology Inc).

**Human hair follicle and skin organ culture**

Normally pigmented anagen VI HFs were microdissected and organ-cultured under serum-free connditions in insulin- and hydrocortisone-supplemented William's E medium (Kloepper *et al.*, 2010; Philpott *et al.*, 1990). Six HF organ cultures were conducted (each derived from a separate patient; total HF number in each culture: 52-132). Two full-thickness human skin organ cultures from two different patients (age 58 and 77) were also conducted as described elsewhere (Bodo *et al.*, 2010; Lu *et al.*, 2007).

Per experiment, HFs were equally divided between those treated with P-cadherin siRNA (test) or scrambled oligos (control). In one culture, culture medium was also supplemented with LiCl 40mM (Sigma, Munich, Germany) (either as the only treatment, or 5-7h after transfection) or TGF $\beta$  neutralizing antibody (monoclonal anti-TGF $\beta$ 1-3 antibody) 5 $\mu$ g/ml (R&D systems, Wiesbaden, Germany) (either the only treatment or simultaneously with the transfection). LiCl was added only once to the culture medium (5-7h after transfection) and HFs were embedded 24h afterwards. TGF $\beta$ -neutralizing antibody was added first, 5-7h after transfection, and a concentration of 5 $\mu$ g/ml was added every day in a four day culture period.

Hair shaft length was measured daily using an inverted binocular microscope (Philpott *et al.*, 1990) and culture medium was replaced immediately after the transfection and then every other day. On days 2 and 4 (and also on day 3 in the two transfection cultures), samples of culture medium were taken for measuring the lactate dehydrogenase (LDH) level as a general cell toxicity parameter in human skin organ culture (Lu *et al.*, 2007). This showed no significant increase in the LDH release of P-cadherin-silenced HFs compared to HFs treated with scrambled oligo-controls after a single transfection, but demonstrated the expected rise in LDH levels after repeated siRNA treatment (data not shown). This indicates minimal toxicity after a single transfection, while repeated transfection carries the expected risk of increased toxicity. 24 hours after the transfection (on day 1 in the one transfection cultures and on day 4 in the 2 transfection cultures) 12-25 HFs from each culture were frozen in liquid nitrogen for RNA extraction and mRNA analysis. The rest of the HFs in each culture were embedded in Shandon Cryomatrix (Pittsburgh, PA, USA) and snap frozen in liquid nitrogen on day 4 of culture. HFs that were treated with LiCl, were embedded 24h after the beginning of treatment.

Five to seven 6µm thick cryosections of organ-cultured human HFs were prepared for subsequent immunohistology, and were stored at -80°C until use.

In the two skin organ cultures, 2mm full-thickness skin punches were transfected with P-cadherin siRNA and control siRNA at day 0 (6 pieces per group) using similar protocol as for HF organ culture. In one culture, 24h after transfection, skin punches were frozen in liquid nitrogen for RNA extraction and mRNA analysis. In the second culture, skin punches were embedded in Shandon Cryomatrix and snap frozen in liquid nitrogen on day 4 of culture. 7µm thick cryosections of skin punches were cut for immunohistological staining.

The efficacy of gene silencing was evaluated using P-cadherin specific immunohistochemistry and Q-PCR, both in the HF and skin organ cultures.

**Immunohistochemistry**

LSAB – peroxidase immunohistology

The cryosections were first air-dried for 10 min and then fixed in acetone at -20°C for another 10 min. After air drying, the slides were washed three times for 5 min in Tris-buffered saline (TBS). Endogenous peroxidase blocking was achieved by putting the slides in 3% hydrogen peroxide for 15 min, followed by three washings with TBS, 5 min each. In the following step, the mouse anti-human P-cadherin monoclonal antibody and mouse anti-human β-catenin monoclonal antibody (both from BD transduction laboratories, Heidelberg, Germany, clones 56 and 14 respectively), rabbit anti-human phospho-β-catenin (Ser33/37/Thr41) (Cell Signaling Technology, Danvers, MA, USA) in 1:50 dilution with antibody diluent (DCS Detection Line, Hamburg, Germany) and mouse anti-human E-cadherin monoclonal antibody (Invitrogen, Darmstadt, Germany, clone HECD1, predilute antibody) were put on the



1  
2  
3 cryosections at 4 °C overnight. After washing three times for 5 min with TBS, sections  
4  
5 were stained with polylink biotinylated secondary antibody (DCS Detection Line) for  
6  
7 20 min at room temperature (RT). After three washings for 5 min with TBS, a 20 min  
8  
9 application of horse radish peroxidase labeled (HRP) avidin biotin complex (DCS  
10  
11 Detection Line) followed, both at RT. Finally, the slides were labelled with 3-amino-9-  
12  
13 ethylcarbazole (DCS ChromoLine, Hamburg, Germany) and counterstained with  
14  
15 haematoxylin with washing steps in between.  
16  
17

18  
19  
20 For the P-cadherin staining, normal breast tissue was used as negative and positive  
21  
22 control (Supplementary Figure S6a). As positive controls we further used normal  
23  
24 breast tissue (for E-cadherin) (Supplementary Figure S6b) and normal epidermis (for  
25  
26 GSK3 $\beta$ ) as previously published (Kovacs *et al.*, 2003; Yamaguchi *et al.*, 2007).  
27  
28 Positive staining of  $\beta$ -catenin in the human HF by the same primary antibody  
29  
30 employed here was previously demonstrated (Tsuji *et al.*, 2001). Positive staining of  
31  
32 phospho- $\beta$ -catenin by the same antibody and with a similar immunoreactivity pattern  
33  
34 as seen here was previously published (Kielhorn *et al.*, 2003; Nakopoulou *et al.*,  
35  
36 2006). Negative controls were performed by deleting the primary antibodies, and by  
37  
38 demonstrating negative immunoreactivity in cell compartments/tissues in accordance  
39  
40 with the literature.  
41  
42  
43  
44  
45

#### 46 **Immunofluorescence**

47  
48 In order to better localize  $\beta$ -catenin and phospho- $\beta$ -catenin expression in the HF and  
49  
50 also in order to demonstrate GSK3 $\beta$  IR, we used also immunofluorescence  
51  
52 techniques. For  $\beta$ -catenin staining, after fixation with acetone and washing with TBS,  
53  
54 cryosections were incubated overnight at 4°C with the mouse anti-human  $\beta$ -catenin  
55  
56 monoclonal antibody (BD transduction laboratories) in 1:50 dilution with TBS,  
57  
58 followed by incubation of 45 min at RT with FITC-labeled goat anti-mouse IgG  
59  
60

(Jackson ImmunoResearch Laboratories, West Grove, PA, USA) diluted 1:200 in TBS and normal goat serum. For phospho- $\beta$ -catenin and GSK3 $\beta$  staining, after washing the slides with phosphate buffered saline (PBS), cryosections were incubated overnight at 4°C with the rabbit anti-human phospho- $\beta$ -catenin (Ser33/37/Thr41) (Cell Signaling Technology) and mouse anti-human GSK3 $\beta$  (BD Transduction Laboratories) in 1:50 and 1:20 dilutions respectively with antibody diluents (DCS Detection Line). This was followed by incubation with FITC-labeled goat anti-mouse and goat anti-rabbit IgG (Jackson ImmunoResearch Laboratories), respectively, for 45 min at RT in 1:200 in antibody diluent (DCS Detection Line). Incubation steps were interspersed with three washes, 5 min each. Then sections were stained with DAPI in a concentration of 1 $\mu$ g/ml (1 min at RT) for identification of cell nuclei.

Since TGF $\beta$ 2 is a recognized key inducer of catagen in human HFs (Soma *et al.*, 2002), TGF $\beta$ 2 expression in HFs treated with P-cadherin siRNA and control siRNA was investigated by using the highly sensitive immunofluorescent TSA technique (Perkin Elmer, Boston, MA, USA) (Roth *et al.*, 1999). Briefly, cryosections of human HFs were incubated with rabbit anti-human TGF $\beta$ 2 (Santa Cruz Biotechnology Inc) as the primary antibody, diluted 1:4000 in Tris-NaCl-Tween Buffer (TNT), overnight at 4°C, followed by incubation with a biotinylated antibody against rabbit IgG (Jackson immunoResearch Laboratories) (1 : 400 in TNT, 45 min, RT). Next, streptavidin–horseradish peroxidase was administered (1 : 100 in TNT, 30 min, RT). Finally, the reaction was amplified by tetramethylrhodamine-tyramide amplification reagent at RT for 5 min (1: 50 in amplification diluent provided in the kit).

### Statistical analysis

All quantitative immunohistochemistry and Hair cycle score (HCS) data were analyzed by *Mann–Whitney test* (GRAPHPAD PRISM version 4.00 for Windows; GraphPad Software, San Diego, CA, USA). Results are expressed as mean  $\pm$  SEM. The results from only different highly comparable experiments using samples from different donors were pooled and statistical differences between groups were also determined by the *Mann–Whitney test*.

All Q-PCR results were analysed by *Student's t test for unpaired samples*. PCR results were normalized to glyceraldehyde 3-phosphate dehydrogenase (GAPDH), peptidylprolyl isomerase A (PPIA) or  $\beta$ -actin.

### Materials and Methods for supplementary data: see Supplement

Apoptosis/proliferation assay, melanin histochemistry, hair cycle staging, quantitative (immuno)histomorphometry, HJMD patient histology, quantitative real-time PCR (Q-PCR), microarray analysis, transmission electron microscopy.

### Conflict of interest

The authors state no conflict of interest

### Acknowledgments

This study was supported by a Minerva fellowship (Max Planck Society) to LS and a grant from Deutsche Forschungsgemeinschaft to RP (DFG Pa 345/12-2). The excellent assistance of Balázs I. Tóth with Q-PCR, Gabriele Scheel with HF histology and Dr. Michael Kinori (Tel-Aviv) with HF organ culture, as well as the histopathological advice of Dr. Christian Rose (Lübeck) are gratefully acknowledged. The authors are also most grateful to our collaborating plastic surgeons (namely, Dr. W. Funk/Munich, Dr. K-H. Bräutigam/Lübeck) for generously providing human scalp

1  
2  
3  
4  
5  
6  
7  
8  
9  
10  
11  
12  
13  
14  
15  
16  
17  
18  
19  
20  
21  
22  
23  
24  
25  
26  
27  
28  
29  
30  
31  
32  
33  
34  
35  
36  
37  
38  
39  
40  
41  
42  
43  
44  
45  
46  
47  
48  
49  
50  
51  
52  
53  
54  
55  
56  
57  
58  
59  
60

skin samples for these studies, and to Drs. Ruth Schmidt-Ullrich (MDC, Berlin) and  
Denis Headon (Roslin Institute, Edinburgh) for critical comments and helpful editorial  
suggestions.

For Review Only

## References

Andl T, Reddy ST, Gaddapara T, Millar SE (2002) WNT signals are required for the initiation of hair follicle development. *Dev Cell* 2:643-653.

Baker CM, Verstuyf A, Jensen KB, Watt FM (2010) Differential sensitivity of epidermal cell subpopulations to beta-catenin-induced ectopic hair follicle formation. *Dev Biol* 343:40-50.

Bandara M, Arun SJ, Allanson M, Widyarini S, Chai Z, Reeve VE (2010) Topical isoflavonoids reduce experimental cutaneous inflammation in mice. *Immunol Cell Biol* 88:727-733.

Ben Amitai D, Lurie R, Laron Z (2006) I-GF-1 signalling controls the hair growth cycle and the differentiation of hair shafts. *J Invest Dermatol* 126:2135; author reply 2135-2136.

Bergman R, Sapir M, Sprecher E (2004) Histopathology of hypotrichosis with juvenile macular dystrophy. *Am J Dermatopathol* 26:205-209.

Bodo E, Kany B, Gaspar E, Knuver J, Kromminga A, Ramot Y, *et al.* (2010) Thyroid-stimulating hormone, a novel, locally produced modulator of human epidermal functions, is regulated by thyrotropin-releasing hormone and thyroid hormones. *Endocrinology* 151:1633-1642.

Fanelli MA, Montt-Guevara M, Diblasi AM, Gago FE, Tello O, Cuello-Carrion FD, *et al.* (2008) P-cadherin and beta-catenin are useful prognostic markers in breast cancer patients; beta-catenin interacts with heat shock protein Hsp27. *Cell Stress Chaperones* 13:207-220.

Faraldo MM, Teuliere J, Deugnier MA, Birchmeier W, Huelsken J, Thiery JP, *et al.* (2007) beta-Catenin regulates P-cadherin expression in mammary basal epithelial cells. *FEBS Lett* 581:831-836.

Fujita M, Furukawa F, Fujii K, Horiguchi Y, Takeichi M, Imamura S (1992) Expression of cadherin cell adhesion molecules during human skin development: morphogenesis of epidermis, hair follicles and eccrine sweat ducts. *Arch Dermatol Res* 284:159-166.

Goodwin M, Yap AS (2004) Classical cadherin adhesion molecules: coordinating cell adhesion, signaling and the cytoskeleton. *J Mol Histol* 35:839-844.

Gottardi CJ, Gumbiner BM (2001) Adhesion signaling: how beta-catenin interacts with its partners. *Curr Biol* 11:R792-794.

Heuberger J, Birchmeier W (2010) Interplay of cadherin-mediated cell adhesion and canonical Wnt signaling. *Cold Spring Harb Perspect Biol* 2:a002915.

Hibino T, Nishiyama T (2004) Role of TGF-beta2 in the human hair cycle. *J Dermatol Sci* 35:9-18.

Hirai Y, Nose A, Kobayashi S, Takeichi M (1989) Expression and role of E- and P-cadherin adhesion molecules in embryonic histogenesis. II. Skin morphogenesis. *Development* 105:271-277.

Huelsken J, Vogel R, Erdmann B, Cotsarelis G, Birchmeier W (2001) beta-Catenin controls hair follicle morphogenesis and stem cell differentiation in the skin. *Cell* 105:533-545.

Indelman M, Bergman R, Lurie R, Richard G, Miller B, Petronius D, *et al.* (2002) A missense mutation in CDH3, encoding P-cadherin, causes hypotrichosis with juvenile macular dystrophy. *J Invest Dermatol* 119:1210-1213.

Indelman M, Eason J, Hummel M, Loza O, Suri M, Leys MJ, *et al.* (2007) Novel CDH3 mutations in hypotrichosis with juvenile macular dystrophy. *Clin Exp Dermatol* 32:191-196.

Jacobs K, Feys L, Vanhoecke B, Van Marck V, Bracke M (2011) P-cadherin expression reduces melanoma growth, invasion, and responsiveness to growth factors in nude mice. *Eur J Cancer Prev* 20:207-216.

Jelani M, Salman Chishti M, Ahmad W (2009) A novel splice-site mutation in the CDH3 gene in hypotrichosis with juvenile macular dystrophy. *Clin Exp Dermatol* 34:68-73.

Kielhorn E, Provost E, Olsen D, D'Aquila TG, Smith BL, Camp RL, *et al.* (2003) Tissue microarray-based analysis shows phospho-beta-catenin expression in malignant melanoma is associated with poor outcome. *Int J Cancer* 103:652-656.

Kim S, Choi IF, Quante JR, Zhang L, Roop DR, Koster MI (2009) p63 directly induces expression of Alox12, a regulator of epidermal barrier formation. *Exp Dermatol* 18:1016-1021.

Kjaer KW, Hansen L, Schwabe GC, Marques-de-Faria AP, Eiberg H, Mundlos S, *et al.* (2005) Distinct CDH3 mutations cause ectodermal dysplasia, ectrodactyly, macular dystrophy (EEM syndrome). *J Med Genet* 42:292-298.

Kloepper JE, Sugawara K, Al-Nuaimi Y, Gaspar E, van Beek N, Paus R (2010) Methods in hair research: how to objectively distinguish between anagen and catagen in human hair follicle organ culture. *Exp Dermatol* 19:305-312.

Kovacs A, Dhillon J, Walker RA (2003) Expression of P-cadherin, but not E-cadherin or N-cadherin, relates to pathological and functional differentiation of breast carcinomas. *Mol Pathol* 56:318-322.

Kuphal F, Behrens J (2006) E-cadherin modulates Wnt-dependent transcription in colorectal cancer cells but does not alter Wnt-independent gene expression in fibroblasts. *Exp Cell Res* 312:457-467.

Kwack MH, Shin SH, Kim SR, Im SU, Han IS, Kim MK, *et al.* (2009) L-Ascorbic acid 2-phosphate promotes elongation of hair shafts via the secretion of insulin-like growth factor-1 from dermal papilla cells through phosphatidylinositol 3-kinase. *Br J Dermatol* 160:1157-1162.

Leibu R, Jermans A, Hatim G, Miller B, Sprecher E, Perlman I (2006) Hypotrichosis with juvenile macular dystrophy: clinical and electrophysiological assessment of visual function. *Ophthalmology* 113:841-847 e843.

Li YH, Zhang K, Ye JX, Lian XH, Yang T (2011) Wnt10b promotes growth of hair follicles via a canonical Wnt signalling pathway. *Clin Exp Dermatol* 36:534-540.

Lovatt M, Bijlmakers MJ (2010) Stabilisation of beta-catenin downstream of T cell receptor signalling. *PLoS One* 5.

Lu Z, Hasse S, Bodo E, Rose C, Funk W, Paus R (2007) Towards the development of a simplified long-term organ culture method for human scalp skin and its appendages under serum-free conditions. *Exp Dermatol* 16:37-44.

Mikkola ML, Costanzo A, Thesleff I, Roop DR, Koster MI (2010) Treasure or artifact: a decade of p63 research speaks for itself. *Cell Death Differ* 17:180-183; author reply 184-186.

Millar SE (2002) Molecular mechanisms regulating hair follicle development. *J Invest Dermatol* 118:216-225.

Muller-Rover S, Peters EJ, Botchkarev VA, Panteleyev A, Paus R (1998) Distinct patterns of NCAM expression are associated with defined stages of murine hair follicle morphogenesis and regression. *J Histochem Cytochem* 46:1401-1410.

Muller-Rover S, Tokura Y, Welker P, Furukawa F, Wakita H, Takigawa M, et al. (1999) E- and P-cadherin expression during murine hair follicle morphogenesis and cycling. *Exp Dermatol* 8:237-246.

Nakopoulou L, Mylona E, Papadaki I, Kavantzias N, Giannopoulou I, Markaki S, et al. (2006) Study of phospho-beta-catenin subcellular distribution in invasive breast carcinomas in relation to their phenotype and the clinical outcome. *Mod Pathol* 19:556-563.

Nelson WJ, Nusse R (2004) Convergence of Wnt, beta-catenin, and cadherin pathways. *Science* 303:1483-1487.

Paredes J, Correia AL, Ribeiro AS, Albergaria A, Milanezi F, Schmitt FC (2007) P-cadherin expression in breast cancer: a review. *Breast Cancer Res* 9:214.

Paus R, Cotsarelis G (1999) The biology of hair follicles. *N Engl J Med* 341:491-497.

Paus R, Foitzik K (2004) In search of the "hair cycle clock": a guided tour. *Differentiation* 72:489-511.

Philpott MP, Green MR, Kealey T (1990) Human hair growth in vitro. *J Cell Sci* 97 ( Pt 3):463-471.

Philpott MP, Sanders DA, Kealey T (1994) Effects of insulin and insulin-like growth factors on cultured human hair follicles: IGF-I at physiologic concentrations is an important regulator of hair follicle growth in vitro. *J Invest Dermatol* 102:857-861.



Radice GL, Ferreira-Cornwell MC, Robinson SD, Rayburn H, Chodosh LA, Takeichi M, *et al.* (1997) Precocious mammary gland development in P-cadherin-deficient mice. *J Cell Biol* 139:1025-1032.

Roth KA, Adler K, Bobrow MN (1999) Enhanced tyramide signal amplification immunohistochemical detection. *J Histochem Cytochem* 47:1644D-1645.

Schneider MR, Schmidt-Ullrich R, Paus R (2009) The hair follicle as a dynamic miniorgan. *Curr Biol* 19:R132-142.

Shimizu H, Morgan BA (2004) Wnt signaling through the beta-catenin pathway is sufficient to maintain, but not restore, anagen-phase characteristics of dermal papilla cells. *J Invest Dermatol* 122:239-245.

Shimomura Y, Wajid M, Kurban M, Christiano AM (2010) Splice site mutations in the P-cadherin gene underlie hypotrichosis with juvenile macular dystrophy. *Dermatology* 220:208-212.

Shimomura Y, Wajid M, Shapiro L, Christiano AM (2008) P-cadherin is a p63 target gene with a crucial role in the developing human limb bud and hair follicle. *Development* 135:743-753.

Shimoyama Y, Hirohashi S, Hirano S, Noguchi M, Shimosato Y, Takeichi M, *et al.* (1989) Cadherin cell-adhesion molecules in human epithelial tissues and carcinomas. *Cancer Res* 49:2128-2133.

Slominski A, Wortsman J, Plonka PM, Schallreuter KU, Paus R, Tobin DJ (2005) Hair follicle pigmentation. *J Invest Dermatol* 124:13-21.

Soma T, Tsuji Y, Hibino T (2002) Involvement of transforming growth factor-beta2 in catagen induction during the human hair cycle. *J Invest Dermatol* 118:993-997.

Sprecher E, Bergman R, Richard G, Lurie R, Shalev S, Petronius D, *et al.* (2001) Hypotrichosis with juvenile macular dystrophy is caused by a mutation in CDH3, encoding P-cadherin. *Nat Genet* 29:134-136.

Stenn KS, Paus R (2001) Controls of hair follicle cycling. *Physiol Rev* 81:449-494.

Tighe A, Ray-Sinha A, Staples OD, Taylor SS (2007) GSK-3 inhibitors induce chromosome instability. *BMC Cell Biol* 8:34.

Tsuji H, Ishida-Yamamoto A, Takahashi H, Iizuka H (2001) Nuclear localization of beta-catenin in the hair matrix cells and differentiated keratinocytes. *J Dermatol Sci* 27:170-177.

Van Mater D, Kolligs FT, Dlugosz AA, Fearon ER (2003) Transient activation of beta-catenin signaling in cutaneous keratinocytes is sufficient to trigger the active growth phase of the hair cycle in mice. *Genes Dev* 17:1219-1224.

Weger N, Schlake T (2005) Igf-I signalling controls the hair growth cycle and the differentiation of hair shafts. *J Invest Dermatol* 125:873-882.



1  
2  
3  
4  
5 Yamaguchi Y, Passeron T, Watabe H, Yasumoto K, Rouzaud F, Hoashi T, *et al.* (2007) The  
6 effects of dickkopf 1 on gene expression and Wnt signaling by melanocytes: mechanisms  
7 underlying its suppression of melanocyte function and proliferation. *J Invest Dermatol*  
8 127:1217-1225.  
9

10 Zhao J, Harada N, Kurihara H, Nakagata N, Okajima K (2011) Dietary isoflavone increases  
11 insulin-like growth factor-I production, thereby promoting hair growth in mice. *J Nutr*  
12 *Biochem* 22:227-233.  
13  
14  
15  
16  
17  
18  
19  
20  
21  
22  
23  
24  
25  
26  
27  
28  
29  
30  
31  
32  
33  
34  
35  
36  
37  
38  
39  
40  
41  
42  
43  
44  
45  
46  
47  
48  
49  
50  
51  
52  
53  
54  
55  
56  
57  
58  
59  
60

Figure legends

Figure 1. Working hypothesis: P-cadherin regulates human hair growth via the canonical Wnt signaling pathway through  $\beta$ -catenin

(a) Presence of P-cadherin. Under physiological conditions,  $\beta$ -catenin is found in epithelial cells either bound to the cytoplasmic domain of classical cadherins (here: P-cadherin) in adherens junctions (AJs), or free in the cytoplasm. In the absence of Wnt ligands, excess cytoplasmic  $\beta$ -catenin is recruited to a destruction complex that contains adenomatous polyposis coli (APC), axins and Glycogen synthase kinase 3 beta (GSK3 $\beta$ ). The destruction complex is responsible for the phosphorylation of  $\beta$ -catenin which is subsequently targeted for proteosomal degradation. In the presence of Wnt ligands, which bind to members of the Frizzled (Fz) receptor families, the destruction complex is inactivated. This leads to an increase of  $\beta$ -catenin molecules in the cytoplasm and translocation into the nucleus, where  $\beta$ -catenin binds to members of the lymphoid enhancer-binding factor 1 (LEF) and T cell factor (TCF) family of transcription factors.  $\beta$ -catenin/LEF/TCF complexes control the expression of genes involved in the control of hair morphogenesis and hair cycling, as well as axin2 and insulin-like growth factor1 (IGF1). For greater simplicity, the reported regulation of P-cadherin by p63 (Shimomura *et al.*, 2008), is not shown here.

(b) Absence of P-cadherin. Canonical Wnt signaling and cadherin-mediated cell adhesion depend on the same cytoplasmic pool of  $\beta$ -catenin (Gottardi and Gumbiner, 2001). P-cadherin absence (by P-cadherin knock-down or in HJMD patients) results in over-degradation of cytoplasmic  $\beta$ -catenin and reduced  $\beta$ -catenin which is available for the normal Wnt signaling within the cells. This results in reduced Wnt target gene expression which control hair follicle growth and cycling, causing premature catagen induction.

$\beta$  -  $\beta$ -catenin;  $\alpha$  -  $\alpha$ -catenin; IC - intracytoplasmic domain of P-cadherin; P-phospho; Ub – ubiquitin; GSK3 $\beta$  - Glycogen synthase kinase 3 beta; IGF-1 - insulin like growth factor 1; APC – adenomatous polyposis coli; LEF1 - lymphoid enhancer-binding factor 1; FZ – Frizzled, CK1a - axin-bound casein kinase 1a (CK1a), Tcf – T-cell factor.

**Figure 2. Constitutive P-cadherin expression and P-cadherin knock-down in normal human hair follicles**

(a) P-cadherin immunoreactivity (IR) by LSAB - peroxidase immunohistology, in the innermost hair matrix (IHM) and the outer root sheath (ORS) of a normal anagen VI human hair follicle (HF).

(b) Significantly reduced *CDH3* transcript steady-state levels in normal catagen HF compared to anagen HF. RNA was extracted from anagen and catagen HF that were cultured for 8 days under the same culture conditions. HF were defined as anagen/catagen according to their macroscopic appearance. \*\*  $p < 0.01$ , *Student's t test for unpaired samples*.

(c-e) Successful P-cadherin knock-down demonstrated on the protein level: P-cadherin IR is reduced in the IHM and ORS of P-cadherin siRNA-treated HF (d), compared to scrambled oligo-treated HF (c). Data were pooled from 2 highly comparable, independent experiments (e). Dotted lines in figure (c) represent reference areas of IR measurement. \*\*\*  $p < 0.001$ , *Mann-Whitney test*,  $n = 17-23$ .

(f) Reduced *CDH3* mRNA level was demonstrated in P-cadherin siRNA treated HF. \*\* $p < 0.01$ , *Student's t test for unpaired samples*.

(g-h) Catagen induction after treatment with P-cadherin siRNA. The graphs represent data pooled from 3 independent experiments after one transfection;  $n = 46-47$  HF in each group. Hair cycle staging was assessed by Ki-67 staining, as well as by quantitative Masson-Fontana histochemistry. Data are presented as hair cycle score (HCS) (g) or as percentage of HF in anagen VI, early, mid or late catagen (h). To calculate the HCS, each anagen VI HF was ascribed to an arbitrary value of 100, early catagen to 200, mid catagen to 300 and late catagen to 400. Values were added per group and divided by the number of HF. Thus, the score represents the mean hair cycle stage of all HF per treatment group. Significance refers to the HCS of control HF (i.e. HF treated with scrambled oligos after 4 days of culture). \*\*\* $p < 0.0001$ , *Mann-Whitney test*.

(i-l) Significantly higher keratinocyte proliferation below Auber's line (dotted line) in HF*s* treated with scrambled oligos (i), compared to P-cadherin siRNA-treated HF*s* (j). Quantification of Ki-67+ keratinocytes was done below Auber's line. A reduced proliferation rate was observed when comparing anagen and catagen HF*s* (l, \*\*\**p*<0.0001, *Mann-Whitney test*, *n*=20-21) and only anagen HF*s* (k, \*\*\**p*<0.001, *Mann-Whitney test*, *n*=11-18) after treatment with either scrambled or P-cadherin siRNAs. Data was pooled from 2 highly comparable, independent experiments.

IHM – innermost hair matrix; DP – dermal papilla; ORS – outer root sheath; HS – hair shaft; IR – immunoreactivity; HF*s* – hair follicles.

**Figure 3. P-cadherin knock-down inhibits hair shaft production in organ culture *in situ***

(a) Reduced hair shaft elongation after P-cadherin silencing. Data was pooled from four highly comparable, independent experiments, with one transfection with P-cadherin siRNA or scrambled oligos at day 0; *n*=107-110 in each group.

(b) No additive effect of repeated knock-down on hair shaft elongation. Data was pooled from two highly comparable, independent experiments, with two transfections with P-cadherin siRNA or scrambled oligos at day 0 and 3 of culture; *n*=63-66 in each group. Note the separation of graphs after the second transfection. Growth rates are expressed as percent difference over day 1. Significance refers to the growth rate of hair follicles on day 4 that had been treated with scrambled oligos. \*\*\**p* <0.0001; \*\**p* <0.01, p-cadherin siRNA vs. scrambled oligos treated HF*s*, *Mann-Whitney test*. Scr – scrambled oligos; P-cad – P-cadherin.

**Figure 4. P-cadherin knock-down reduces Insulin-like growth factor 1 (IGF-1) and increases transforming growth factor  $\beta$ 2 (TGF $\beta$ 2) expression**

**(a)** Reduced intrafollicular insulin like growth factor 1 (IGF-1) transcript level in the P-cadherin siRNA treated hair follicles (HFs) compared to scrambled oligo-treated HFs. \* $p < 0.05$ , *Student's t test for unpaired samples*.

**(b)** Increased intrafollicular transforming growth factor  $\beta$ 2 (TGF $\beta$ 2) expression after P-cadherin silencing. The graph represents data pooled from three highly comparable, independent experiments in which HFs were transfected once at day 0 with P-cadherin siRNA or scrambled oligos; \*\*  $p < 0.01$ , *Mann-Whitney test*,  $n = 25-35$ . One of the experiments demonstrated higher but not significant TGF $\beta$ 2 expression in the P-cadherin siRNA treated HFs compared to scrambled oligos treated ones (the results became significant when the data was pooled).

**(c)** Increased intrafollicular TGF $\beta$ 2 expression after P-cadherin silencing. The graph represents data obtained from one experiment in which HFs were transfected twice, at day 0 and 3 of culture. \*\*\*  $p < 0.0001$ , *Mann-Whitney test*,  $n = 8-10$ .

**(d)** Higher TGF $\beta$ 2 protein immunoreactivity in the outer root sheath of the P-cadherin siRNA treated HFs. The dotted lines in the left picture represent the area of measurement and evaluation.

IR – immunoreactivity; ORS – outer root sheath; IGF-1 – insulin like growth factor 1; TGF $\beta$ 2 – transforming growth factor beta 2.

**Figure 5. P-cadherin knock-down increases degradation of  $\beta$ -catenin and reduces expression of  $\beta$ -catenin target genes**

**(a-c)** Significantly reduced  $\beta$ -catenin immunoreactivity (IR) in the innermost hair matrix (IHM) and in other hair follicle (HF) keratinocytes below Auber's line following P-cadherin silencing. Data was pooled from two highly comparable experiments. The immunohistomorphometric analysis graph represents the intensity of immunofluorescence (IF) below the Auber's line (dotted line). \*\*\*  $p < 0.0001$ , *Mann-Whitney* test,  $n = 19-23$ .

**(d-g)** Significantly increased glycogen synthase kinase 3 beta (GSK3 $\beta$ ) and phospho- $\beta$ -catenin IR in the IHM. For GSK3 $\beta$  and phospho- $\beta$ -catenin IR, the graphs represent data taken from two highly comparable experiments in which HFs were transfected once with P-cadherin siRNA or scrambled oligos. Evaluation was done by quantification of IF staining in the IHM with either an anti-phospho- $\beta$ -catenin or an anti-GSK3 $\beta$  antibody (For phospho- $\beta$ -catenin, \*\*\* $p < 0.001$ ,  $n = 17-18$ ; For GSK3 $\beta$  \*\*\* $p < 0.001$ ,  $n = 16-21$ ; *Mann-Whitney* test). All data include anagen and catagen HFs.

**(h,k)** *Axin2* mRNA levels are significantly down-regulated in HFs treated with P-cadherin siRNAs (h). Culturing siRNA-treated HFs with lithium chloride (LiCl), significantly reversed the effect of P-cadherin silencing on *Axin2* transcript level (k). \*\* $p < 0.01$ , \* $p < 0.05$ , *Student's t test for unpaired samples*.

**(i-j)** Phospho- $\beta$ -catenin IR in HFs treated with either scrambled oligos, P-cadherin siRNA, P-cadherin siRNA+ LiCl or LiCl. Note the significant reduction in phospho- $\beta$ -catenin IR after simultaneous treatment with LiCl and P-cadherin siRNA (\* $p < 0.05$ , \*\* $p < 0.01$ , \*\*\* $p < 0.001$ , *Mann-Whitney* test,  $n = 8-11$ ).

GSK3 $\beta$  - Glycogen synthase kinase 3 beta; IHM – innermost hair matrix; DP – dermal papilla; P-  $\beta$ -catenin – phospho- $\beta$ -catenin; LiCl – lithium chloride; Scr – scrambled; P-cad – P-cadherin.

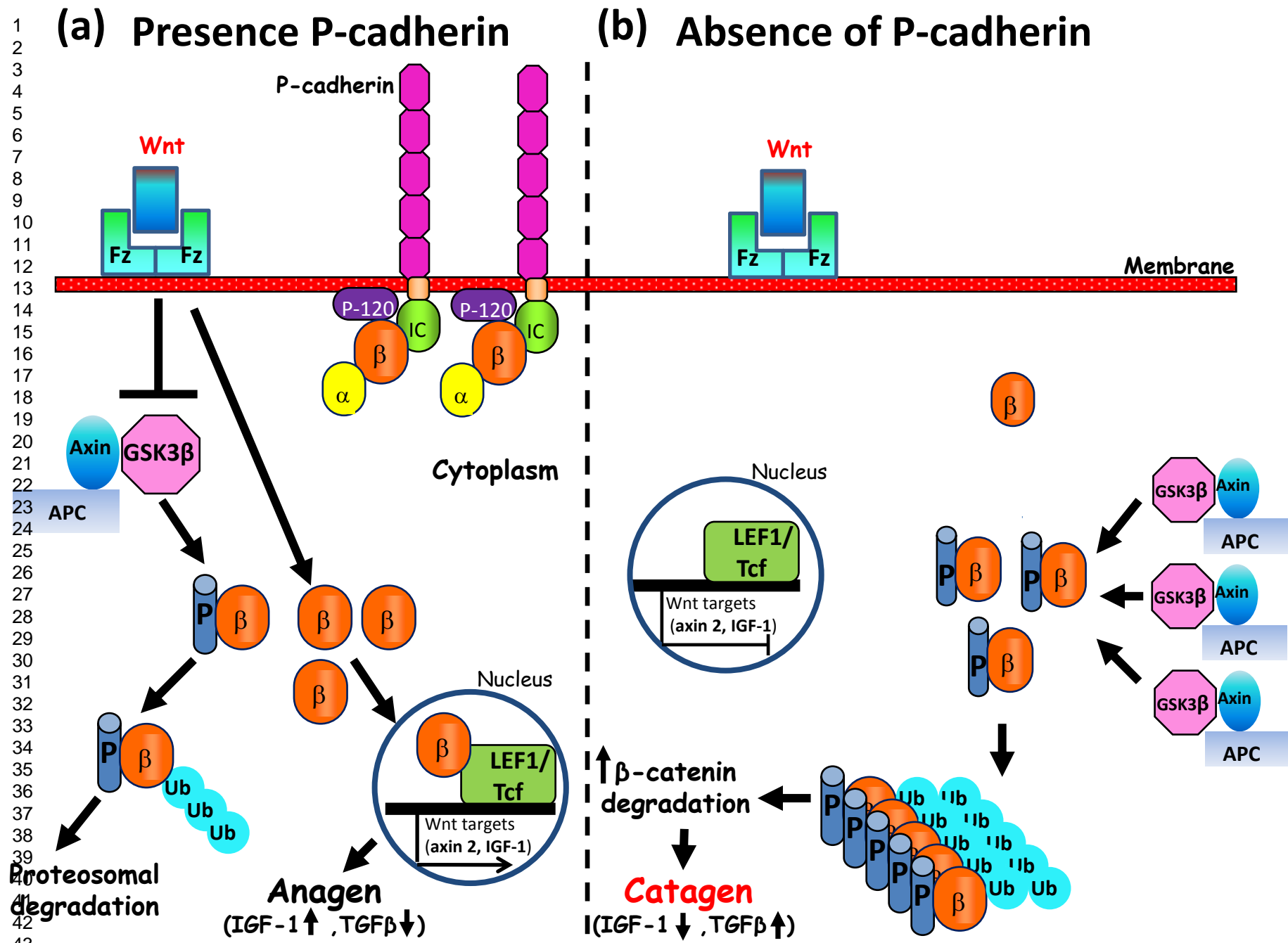
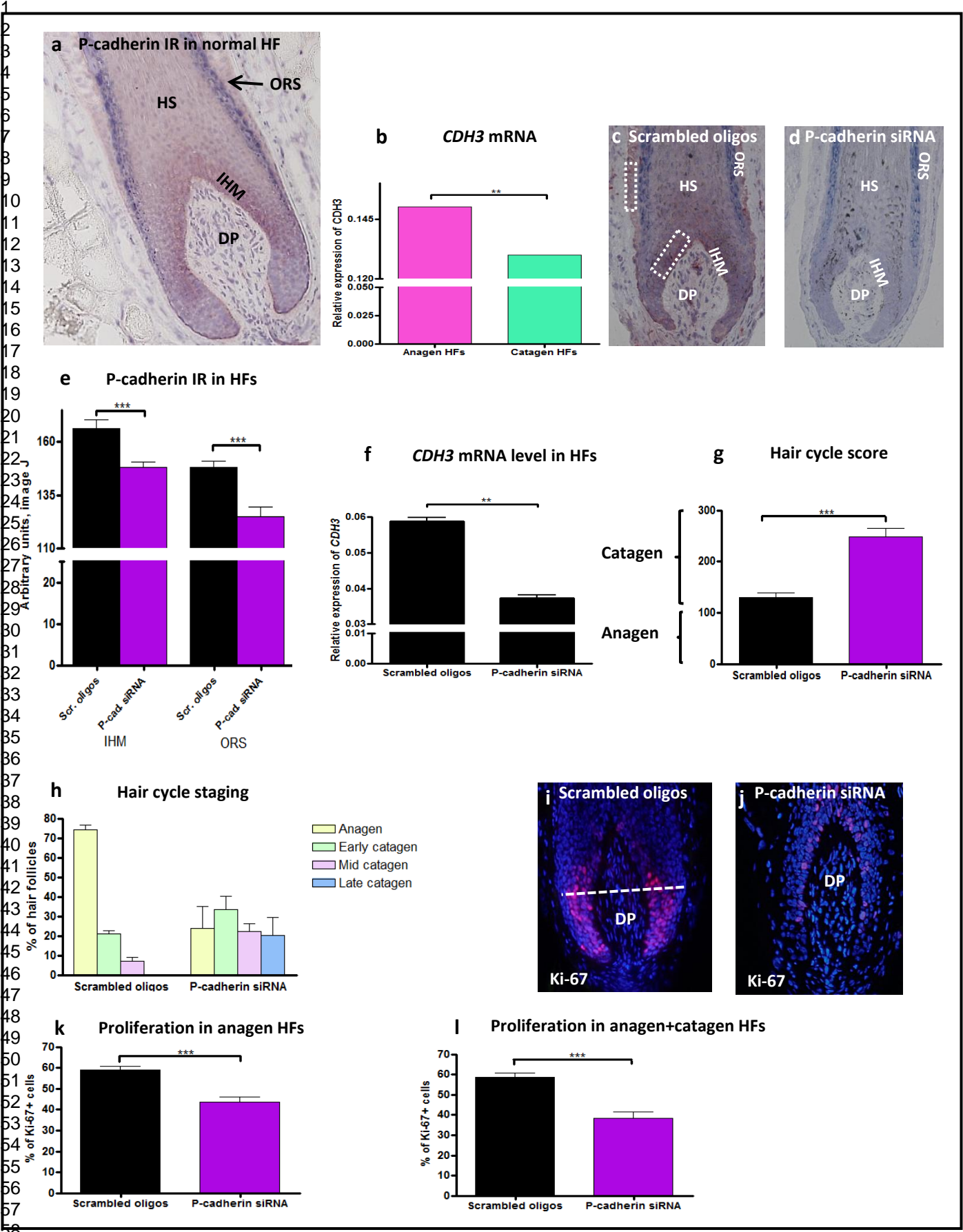


Figure 2





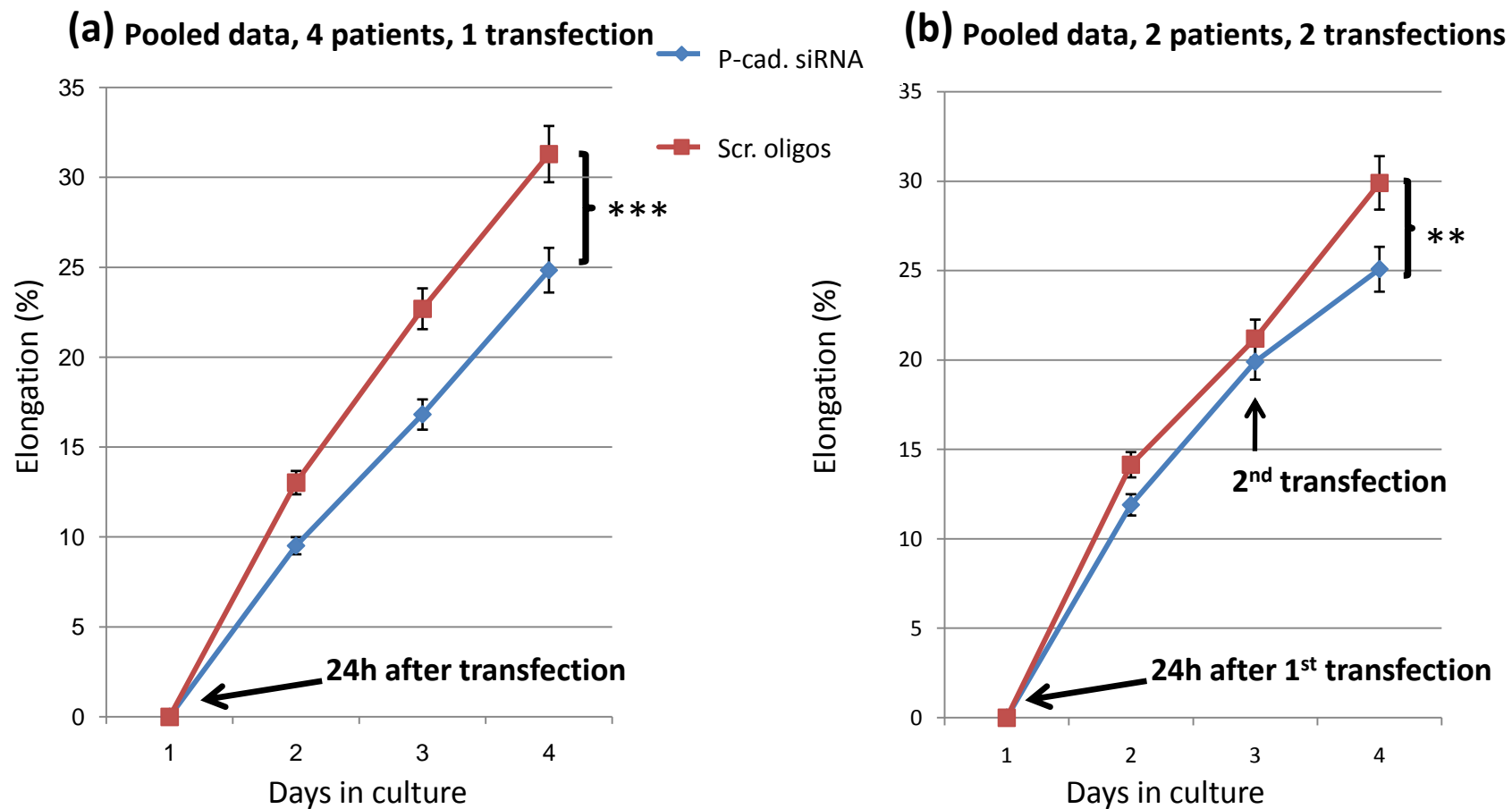
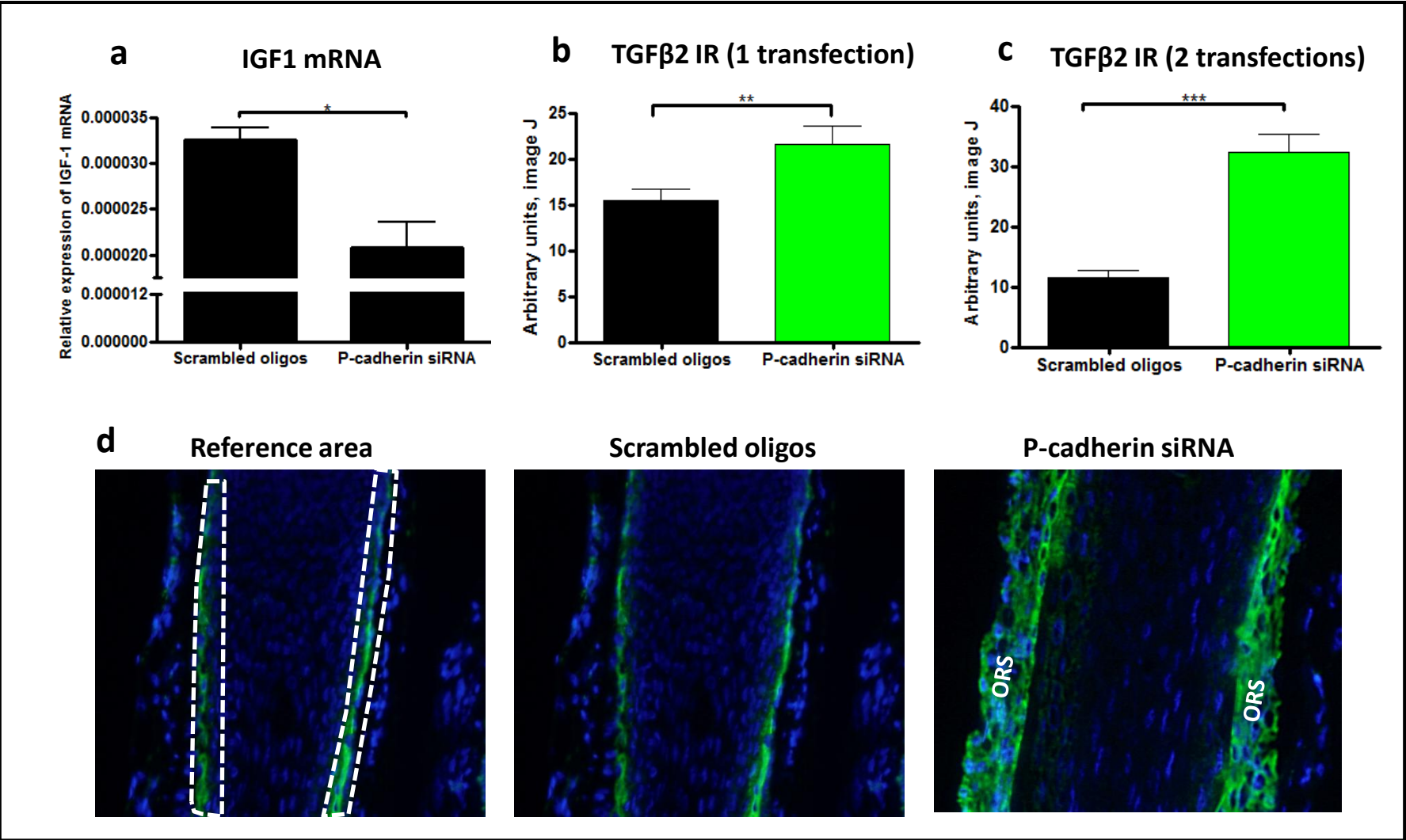
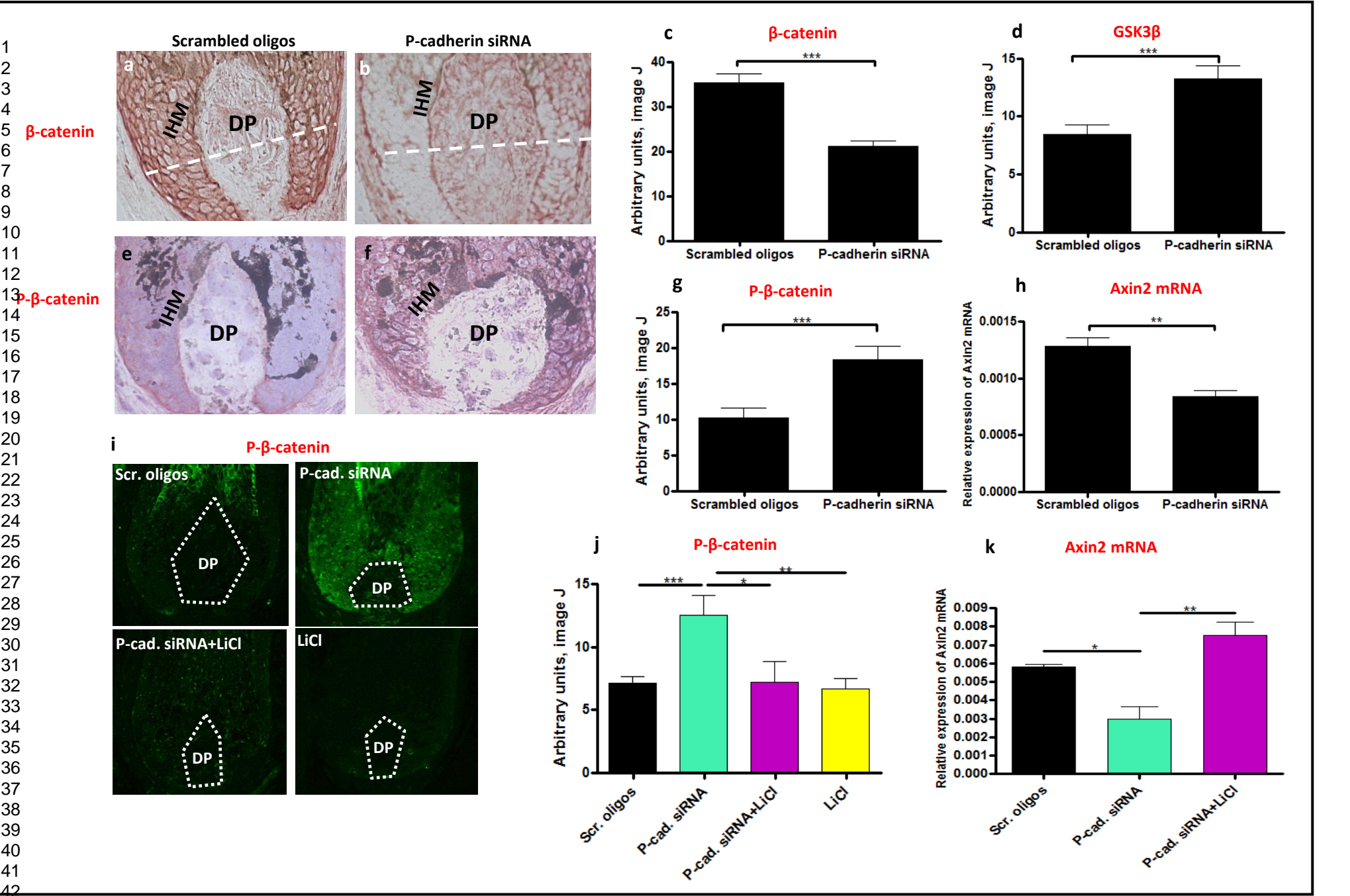
**Figure 3**

Figure 4





**Supplementary data**

**Supplementary Materials and Methods**

**Apoptosis/proliferation assay**

In order to compare degree of proliferation and apoptosis of hair follicles (HFs) in the two treatment groups, double immunolabelling of Ki-67 mouse anti-Ki-67 antiserum (DAKO, Hamburg, Germany) and TUNEL (ApopTag Fluorescein In Situ Apoptosisdetection kit; Millipore, Berlin, Germany) was performed as described previously (Bodo *et al.*, 2004; Foitzik *et al.*, 2000; Kloepper *et al.*, 2008; Peters *et al.*, 2006).

**Melanin histochemistry**

In order to highlight the characteristic, catagen-associated switch-off of follicular melanogenesis (Stenn and Paus, 2001; Tobin *et al.*, 1999), Masson–Fontana histochemistry was employed (Kloepper *et al.*, 2010). Briefly, cryosections were air dried and fixed in ethanol-acetic acid. The sections were washed in Tris-buffered saline (TBS) and distilled water several times. Cryosections were treated with ammoniacal silver solution (Fluka, Seelze, Germany) for 40 min at 56°C in the dark. After washing in distilled water, the sections were treated with 5% aqueous sodium thiosulphate (Merck, Darmstadt, Germany) for 1 min. Then, the sections were washed in running tap water for 3 min and were counterstained with haematoxylin for 45 seconds. After washing in distilled water, sections were dehydrated and mounted in Eukitt (O. Kindler, Freiburg, Germany).

**Hair cycle staging**

Based on proliferation and apoptosis indices in combination with HF morphology and degree of pigmentation by Masson Fontana staining, we determined the stage of each HF (anagen, early catagen, mid catagen, late catagen) and conducted the hair cycle score (HCS) of the two treatment groups, as described previously (Foitzik *et al.*, 2006; Kloepper *et al.*, 2010). For statistical analysis, anagen VI HFs were arbitrarily attributed a score of 100, HFs in early catagen a score of 200, in mid-catagen of 300 and in late catagen of 400. The sum of scores

per group was then divided by the number of investigated HFs (Foitzik *et al.*, 2006). The mean value of these scores therefore is a reliable indicator of the mean HF stage that had been reached on average by a large population of HFs during organ culture.

### Quantitative (immuno)histomorphometry

The immunoreactivity of the different immunohistology protocols and the relative blackness of Masson-Fontana-stained sections was compared between test and control sections in well-defined reference areas by quantitative histomorphometry, as previously described (Peters *et al.*, 2005) using NIH IMAGE software (NIH, Bethesda, MD, USA). For this, the HF was divided anatomically into 4 reference compartments (outer root sheath (ORS); pre-cortical hair matrix (HM); innermost hair matrix (IHM); HM below Auber's line).

### HJMD patient histology

Scalp skin sections stained with Hematoxylin Eosin (H&E) and hair shaft samples of one 5 year old female HJMD patient, obtained for diagnostic purposes after informed consent in the context of an earlier study (Sprecher *et al.*, 2001), were evaluated by light microscopy. Due to the extreme rarity of this syndrome and the difficulty to justify biopsy taking in these pediatric patients, this was the only histological sample available to us for analysis.

### Quantitative Real-Time PCR (Q-PCR)

Q-PCR was performed on an ABI Prism 7000 sequence detection system (Applied Biosystems/Life Technologies, Foster City, CA, USA) using the 5' nuclease assay as detailed in previous reports (Bodo *et al.*, 2005; Dobrosi *et al.*, 2008; Toth *et al.*, 2009). Total RNA was extracted from whole organ cultured HFs using TRIreagent (Applied Biosystems/Life Technologies) and digested with recombinant RNase-free DNase-1 (Applied Biosystems) according to the manufacturer's protocol. After isolation, 1µg of total RNA was reverse-transcribed into cDNA by using High Capacity cDNA kit (Applied Biosystems) following the manufacturer's protocol. PCR amplification was performed by using specific TaqMan primers and probes (Applied Biosystems, assay IDs: Hs00999915\_m1 for human CDH3, Hs00610344\_m1 for human axin2, Hs01547656\_m1 for human IGF-1, Hs00427788\_m1 for

KRT36, Hs01596219\_g1 for KRT37 and Hs00263692\_m1 for KRT84). As internal housekeeping gene controls, transcripts of glyceraldehyde 3-phosphate dehydrogenase (GAPDH), peptidylprolyl isomerase A (PPIA) or  $\beta$ -actin were determined (Assay IDs: Hs99999903 for human ACTB, Hs99999904 for human PPIA and Hs99999905\_m1 for human GAPDH). The amount of the above mentioned transcripts was normalized to those of the control genes using the  $\Delta$ CT method.

**Microarray analysis**

Gene expression analysis was performed by using Human Whole Genome Oligo Microarray® (44K) (Agilent Technologies, Santa Clara, CA, USA). Total RNA was isolated using miRNeasy kit (Qiagen, Hilden, Germany) according to the manufacturer's protocol, and the isolated RNA was quality-checked by Agilent 2100 Bioanalyzer platform (Agilent Technologies) and Nanodrop-1000 Spectrophotometer (NanoDrop/Thermo Scientific, Wilmington, DE, USA). To produce Cy3- and Cy5-labeled cRNA, the Agilent Quick Amp Labeling Kit (Agilent Technologies) was used following the manufacturer's protocol. The hybridization procedure was performed according to the Two-color Microarray-Based Gene Expression Analysis (Quick Amp Labeling) protocol using Agilent Gene Expression Hybridization Kit and fluorescence signals were detected by an Agilent Microarray Scanner (Agilent Technologies).

**Transmission Electron Microscopy (TEM)**

Representative P-cadherin siRNA and scrambled oligos treated HF's were fixed in Karnovsky's fixative overnight at 4 °C as previously described (Tobin *et al.*, 1998), post-fixed in 1% OsO4 (0.1M phosphate buffer, pH 7.4) for 1 h, dehydrated in an ethanol series and embedded in Polybed (Polyscience, Warrington, Pa, USA). Semi-thin sections (0.5 $\mu$ m) were stained with toluidine blue and ultra-thin sections (0.1 $\mu$ m) were stained with saturated uranyl acetate and lead citrate and were examined using a Hitach H-7650 (Tokyo, Japan) electron microscope.



**Supplementary Figure S1. Clinical and histological characteristics of HJMD patients**

**(a)** Both hypotrichosis with juvenile macular dystrophy (HJMD) and ectrodactyly and macular dystrophy (EEM) syndromes result from the same or similar mutations in the *CDH3* gene. The patients are suffering from sparse and short hair as well as progressive macular degeneration leading to blindness during the second decade of life (Shimomura *et al.*, 2008; Sprecher *et al.*, 2001). In EEM, patients have an additional feature of ectrodactyly with split hand and foot malformation, while HJMD patients show normal limb development (Shimomura *et al.*, 2010; Shimomura *et al.*, 2008). The reasons for phenotypic disparity between HJMD and EEM syndromes are not known, although co-inheritance of a mutation in a neighboring gene such as *CDH1* (encoding E-cadherin) or in modifier genes has been postulated (Kjaer *et al.*, 2005; Shimomura *et al.*, 2008).

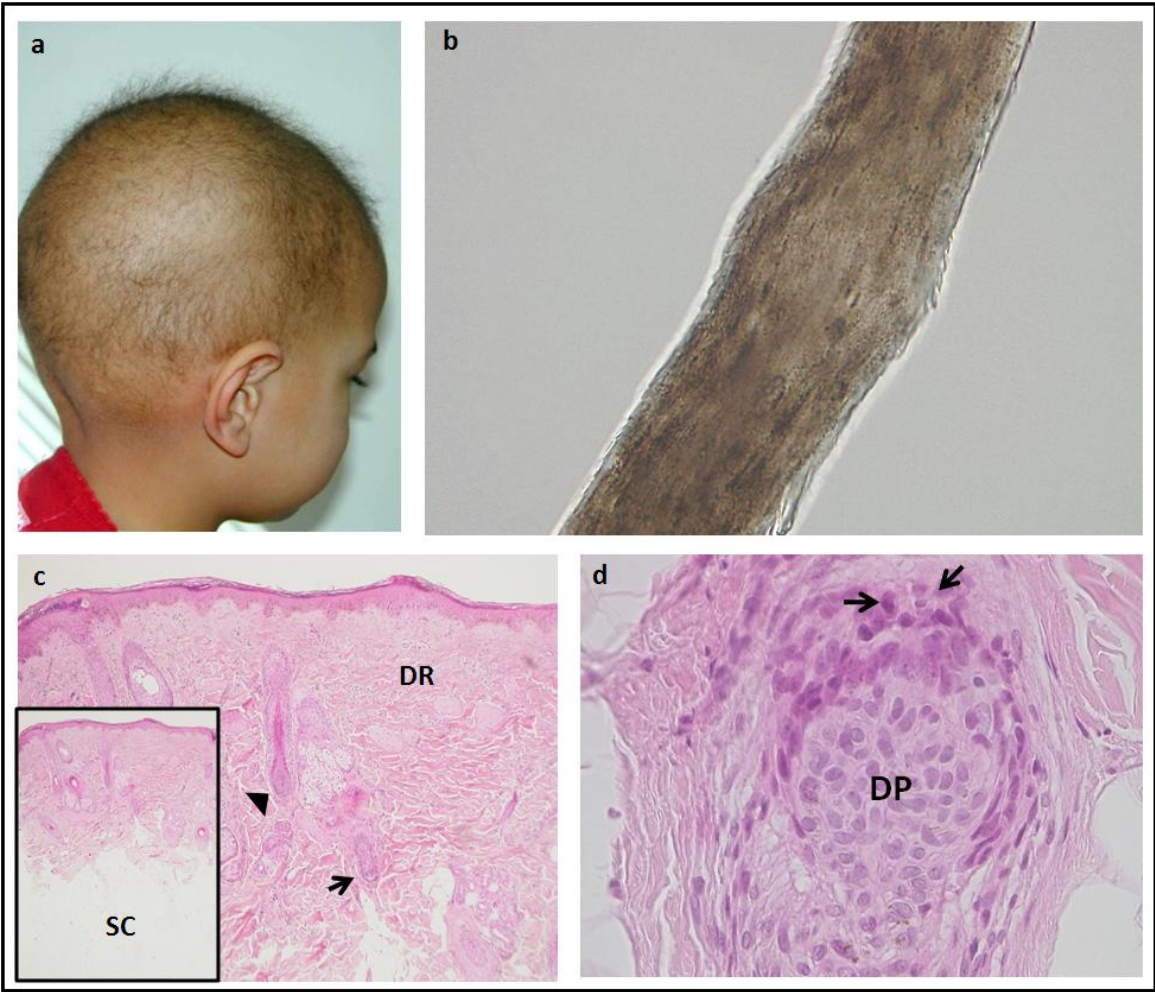
**(b)** Abnormal hair shaft of HJMD patient with pseudomonilethrix appearance and disorganized hair shaft cuticula. Pseudomonilethrix, pili torti, longitudinal ridging, and abnormal hair shaft scaling and folding are recognized in HJMD patients (Bergman *et al.*, 2004).

**(c)** Scalp skin biopsy of HJMD patient (H&E) shows catagen (arrow) and vellus (arrow head) hair follicles (HFs) (H&E, magnification = x40). Insert demonstrates absence of terminal HFs in the subcutaneous tissue.

**(d)** Mid catagen HF of HJMD patient at high magnification (H&E, magnification = x400). The arrows point to karyorhexis, indicating HF dystrophy.

DP – dermal papilla; SC - subcutaneous tissue; DR – dermis.

**Supplementary Figure S1**





**Supplementary Figure S2. Normal P-cadherin expression in human epidermis and P- and E-cadherin expression in human skin punches and hair follicles after P-cadherin knock-down**

**(a)** P-cadherin expression in normal human epidermis. The dotted line represents the dermal-epidermal junction.

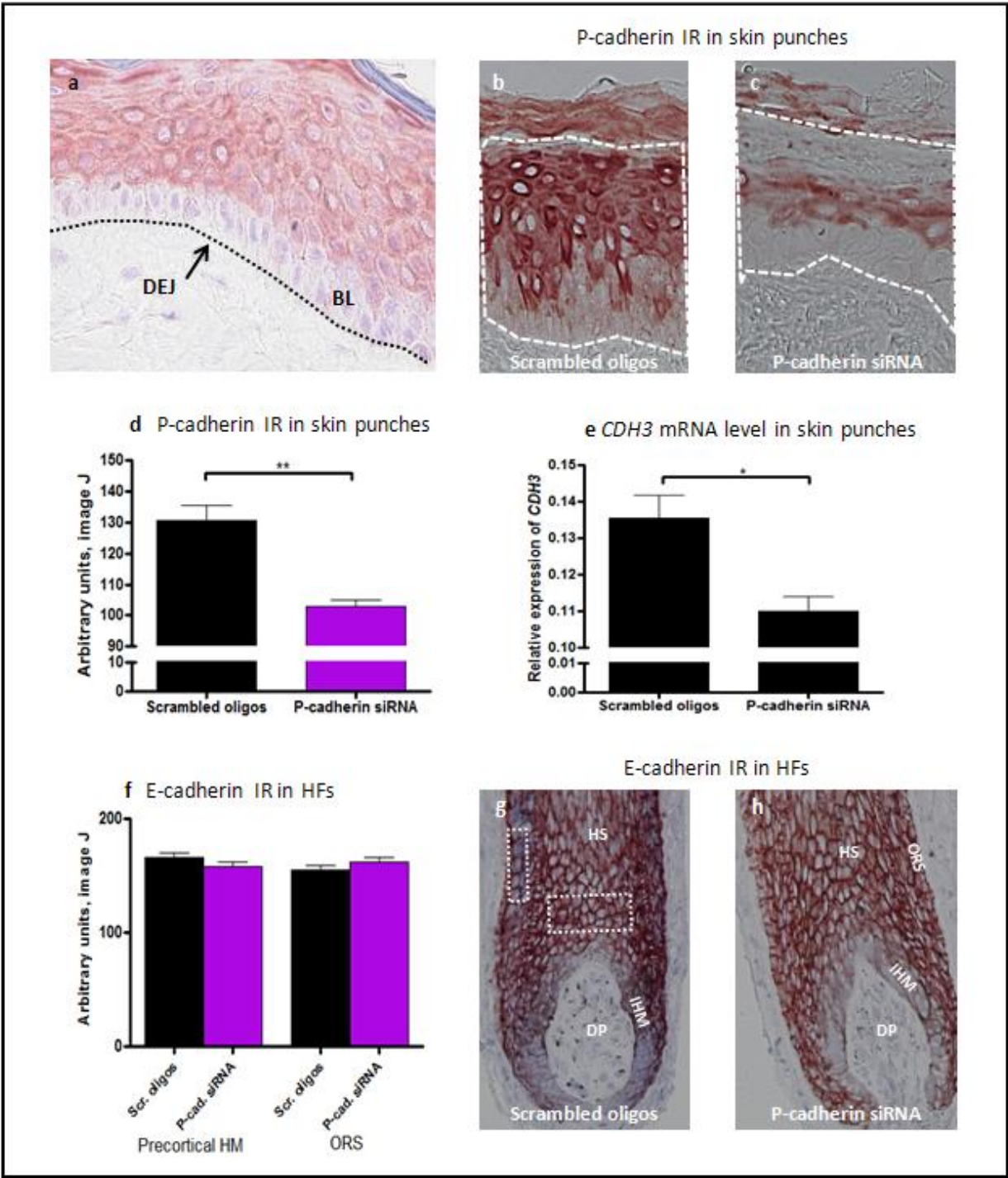
**(b-d)** Reduced P-cadherin immunoreactivity (IR) in the epidermis of 2mm skin punches treated with P-cadherin siRNA, compared to scrambled oligos treated skin punches. \*\* $p < 0.001$ , *Mann Whitney* test,  $n=6$ . Note some remnant P-cadherin expression in the spinous layer of the epidermis following P-cadherin knock-down (c). Dotted lines encircle all epidermal layers, taken as reference area.

**(e)** Reduced CDH3 mRNA level was demonstrated in P-cadherin siRNA treated skin punches. \* $p < 0.05$ , *Student's t test for unpaired samples*.

**(f-h)** No significant change in E-cadherin IR was found in transfected hair follicles. Dotted lines represent reference areas of measurement. Note the diffuse expression of E-cadherin in the human follicular keratinocytes, except in the innermost hair matrix (h).

IHM – innermost hair matrix; DP – dermal papilla; ORS – outer root sheath; HS – hair shaft; HM – hair matrix; IR – immunoreactivity; HFs – hair follicles; DEJ – dermal epidermal junction; BL – basal layer; Scr – scrambled oligos; P-cad – P-cadherin.

Supplementary Figure S2



**Supplementary Figure S3. P-cadherin knock-down results in keratin clumps inside pre-cortical hair matrix keratinocytes**

Ultrastructural analyses by Transmission Electron Microscopy of P-cadherin siRNA treated hair follicle (HF) (a, c, e) compared with scrambled oligos treated one (b, d, f).

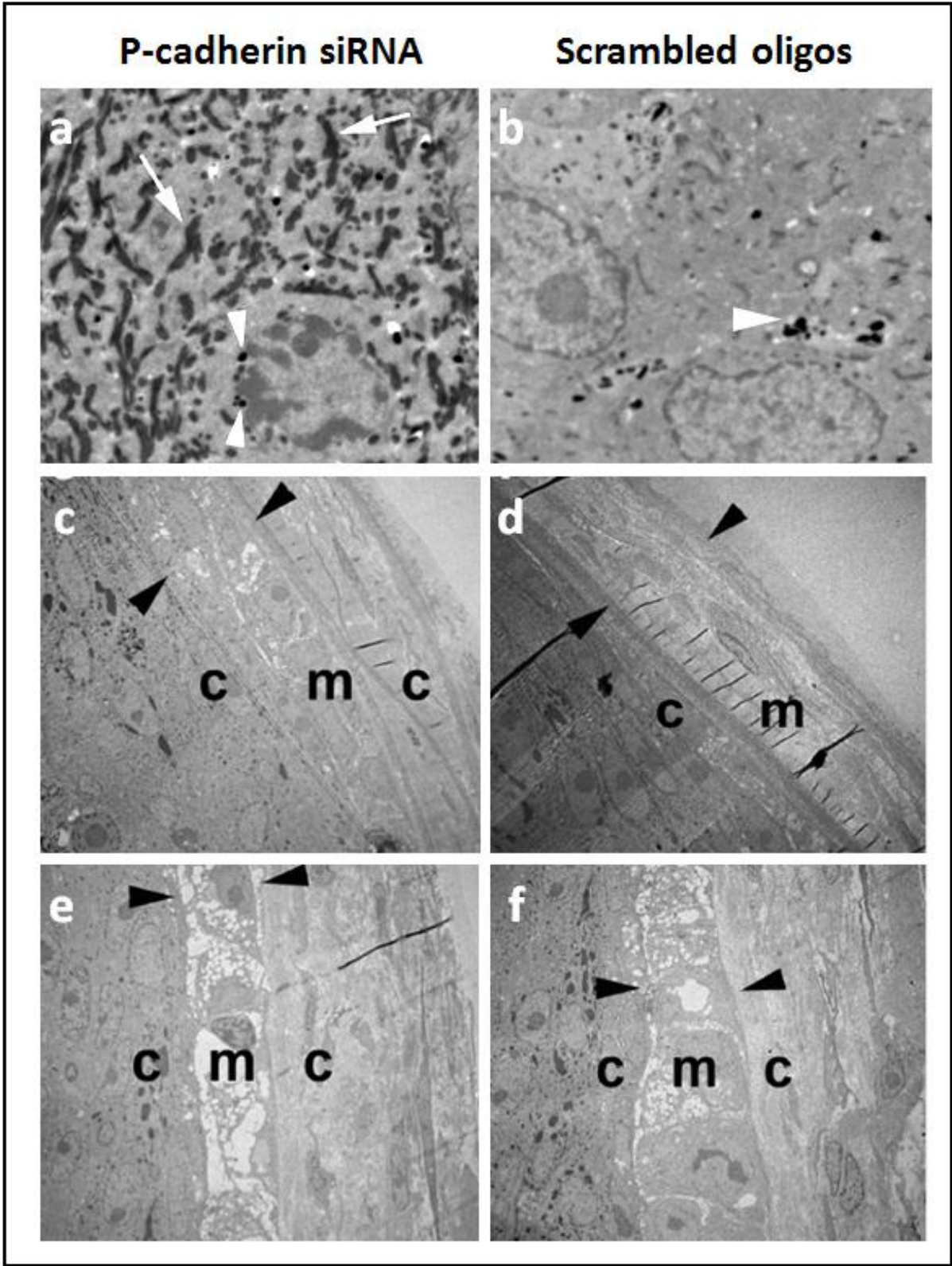
**(a)** Accumulation of massive keratin clumps inside the cytoplasm of the keratinocytes in the precortical hair matrix (white arrows). The white arrowheads indicate melanin granules inside a melanocyte in the hair follicle (HF) pigmentary unit.

**(b)** No evidence of keratin clumps in the precortical hair matrix keratinocytes of a scrambled oligos treated HF. White arrowhead indicates melanin granules inside a keratinocyte.

**(c-f)** Demonstration of the precortical hair matrix region (c-d) in P-cadherin siRNA treated HF (c) and scrambled oligos treated HF (d), and of the proximal hair shaft (e-f) in P-cadherin siRNA treated HF (e) and scrambled oligos treated HF (f). The black arrowheads indicate the borderline between the cortex and the medulla of the hair shaft. Note the narrower intercellular space in P-cadherin siRNA treated HF compared to scrambled oligos treated HF. However, no difference was found in the appearance of both the cortex and the medulla.

c – cortex; m – medulla.

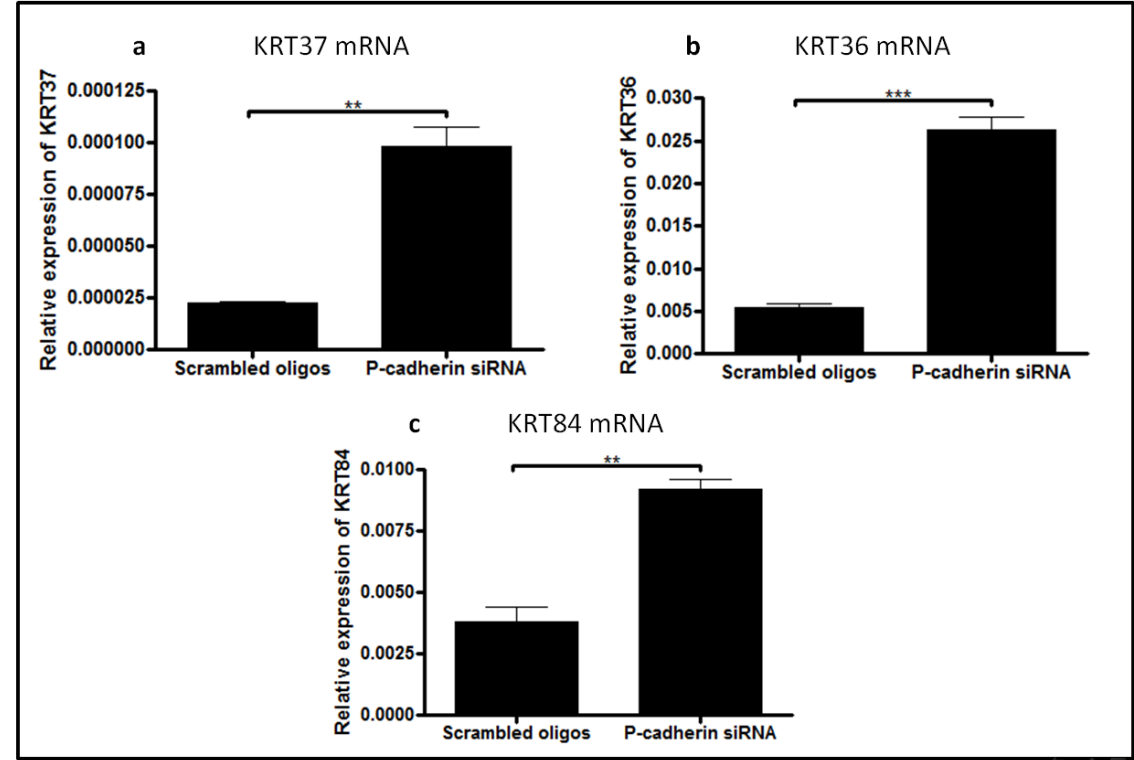
Supplementary Figure S3



**Supplementary Figure S4. Several hair keratins are upregulated by P-cadherin silencing**

Q-PCR analysis revealed upregulation of three specific hair keratins (KRT36/37/84) steady state transcript levels in P-cadherin silenced hair follicles (HFs) compared to scrambled oligos treated HFs, in three different patients, both after one and two transfections with P-cadherin siRNA vs. scrambled oligos. The graphs represent the results in one representative patient for each hair keratin mRNA level. All the three keratins were statistically significant upregulated in the three patients, except one patient that did not show significant upregulation of KRT36. \*\*\*p<0.001; \*\*p<0.01, *Student's t test for unpaired samples*.

**Supplementary Figure S4**





**Supplementary Figure S5. Transforming growth factor beta (TGFβ)-neutralizing antibody partially restores the effects of P-cadherin silencing on human hair growth**

**(a)** Hair shaft elongation measurements of P-cadherin siRNA, P-cadherin siRNA + transforming growth factor β (TGFβ) neutralizing antibody (NA), and hair follicles (HFs) treated only with TGFβ neutralizing antibody; compared to scrambled (Scr) oligo-treated HFs. \*\*\*p<0.001, \*\*p<0.01, *Mann–Whitney* test, n=12-21.

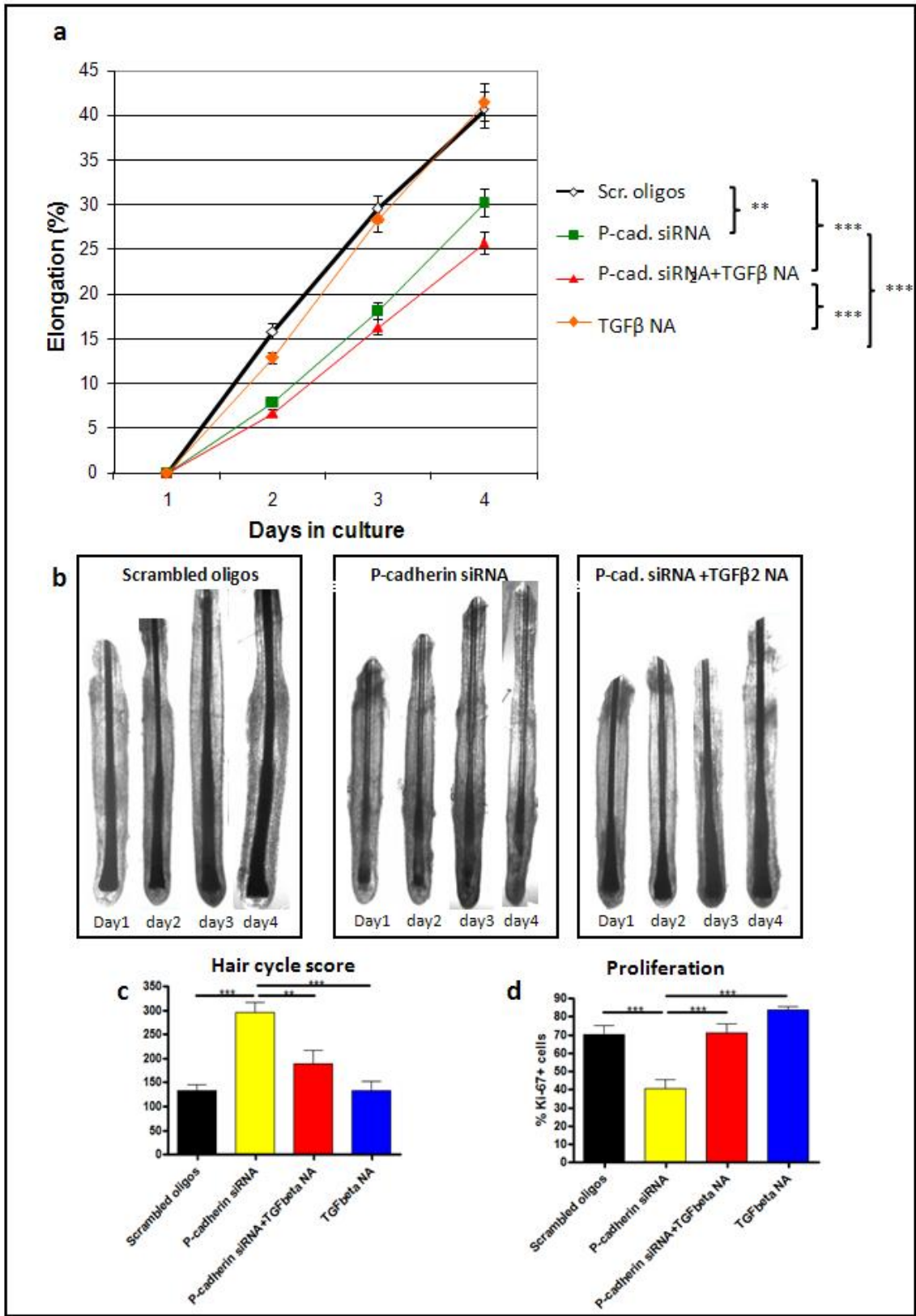
**(b)** Photodocumentation of one characteristic HF per group over a culture period of 4 days.

**(c)** Hair cycle score corresponding to (b). \*\*\*p<0.001, \*\*p>0.01, *Mann–Whitney* test, n=12-21.

**(d)** Ki-67 analysis of hair matrix corresponding to (b). \*\*\*p<0.001, *Mann–Whitney* test, n=12-21.

NA – neutralizing antibody; TGFβ2 - transforming growth factor beta 2; Scr – scrambled; P-cad – P-cadherin.

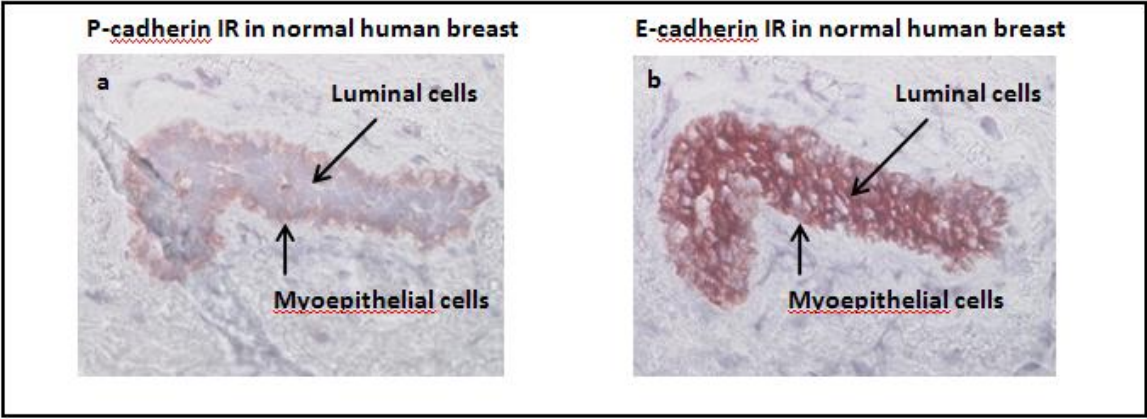
Supplementary Figure S5



**Supplementary Figure S6. Normal P- and E-cadherin expression in human breast tissue**

- (a) P-cadherin positive immunoreactivity (IR) in the myoepithelial cells and negative IR in the luminal epithelium, in normal breast tissue as positive and negative control.
- (b) E-cadherin positive IR in both the myoepithelial and the luminal cells in normal breast tissue as a positive control.

**Supplementary Figure S6**





## Supplementary References

Bergman R, Sapir M, Sprecher E (2004) Histopathology of hypotrichosis with juvenile macular dystrophy. *Am J Dermatopathol* 26:205-209.

Bodo E, Biro T, Telek A, Czifra G, Griger Z, Toth BI, *et al.* (2005) A hot new twist to hair biology: involvement of vanilloid receptor-1 (VR1/TRPV1) signaling in human hair growth control. *Am J Pathol* 166:985-998.

Bodo E, Kovacs I, Telek A, Varga A, Paus R, Kovacs L, *et al.* (2004) Vanilloid receptor-1 (VR1) is widely expressed on various epithelial and mesenchymal cell types of human skin. *J Invest Dermatol* 123:410-413.

Dobrosi N, Toth BI, Nagy G, Dozsa A, Geczy T, Nagy L, *et al.* (2008) Endocannabinoids enhance lipid synthesis and apoptosis of human sebocytes via cannabinoid receptor-2-mediated signaling. *FASEB J* 22:3685-3695.

Foitzik K, Krause K, Conrad F, Nakamura M, Funk W, Paus R (2006) Human scalp hair follicles are both a target and a source of prolactin, which serves as an autocrine and/or paracrine promoter of apoptosis-driven hair follicle regression. *Am J Pathol* 168:748-756.

Foitzik K, Lindner G, Mueller-Roever S, Maurer M, Botchkareva N, Botchkarev V, *et al.* (2000) Control of murine hair follicle regression (catagen) by TGF-beta1 in vivo. *FASEB J* 14:752-760.

Kjaer KW, Hansen L, Schwabe GC, Marques-de-Faria AP, Eiberg H, Mundlos S, *et al.* (2005) Distinct CDH3 mutations cause ectodermal dysplasia, ectrodactyly, macular dystrophy (EEM syndrome). *J Med Genet* 42:292-298.

Kloepper JE, Hendrix S, Bodo E, Tiede S, Humphries MJ, Philpott MP, *et al.* (2008) Functional role of beta 1 integrin-mediated signalling in the human hair follicle. *Exp Cell Res* 314:498-508.

Kloepper JE, Sugawara K, Al-Nuaimi Y, Gaspar E, van Beek N, Paus R (2010) Methods in hair research: how to objectively distinguish between anagen and catagen in human hair follicle organ culture. *Exp Dermatol* 19:305-312.

Peters EM, Hansen MG, Overall RW, Nakamura M, Pertile P, Klapp BF, *et al.* (2005) Control of human hair growth by neurotrophins: brain-derived neurotrophic factor inhibits hair shaft elongation, induces catagen, and stimulates follicular transforming growth factor beta2 expression. *J Invest Dermatol* 124:675-685.

Peters EM, Stieglitz MG, Liezman C, Overall RW, Nakamura M, Hagen E, *et al.* (2006) p75 Neurotrophin Receptor-Mediated Signaling Promotes Human Hair Follicle Regression (Catagen). *Am J Pathol* 168:221-234.

Shimomura Y, Wajid M, Kurban M, Christiano AM (2010) Splice site mutations in the P-cadherin gene underlie hypotrichosis with juvenile macular dystrophy. *Dermatology* 220:208-212.

Shimomura Y, Wajid M, Shapiro L, Christiano AM (2008) P-cadherin is a p63 target gene with a crucial role in the developing human limb bud and hair follicle. *Development* 135:743-753.

Sprecher E, Bergman R, Richard G, Lurie R, Shalev S, Petronius D, *et al.* (2001) Hypotrichosis with juvenile macular dystrophy is caused by a mutation in CDH3, encoding P-cadherin. *Nat Genet* 29:134-136.

Stenn KS, Paus R (2001) Controls of hair follicle cycling. *Physiol Rev* 81:449-494.

1  
2  
3  
4  
5  
6  
7  
8  
9  
10  
11  
12  
13  
14  
15  
16  
17  
18  
19  
20  
21  
22  
23  
24  
25  
26  
27  
28  
29  
30  
31  
32  
33  
34  
35  
36  
37  
38  
39  
40  
41  
42  
43  
44  
45  
46  
47  
48  
49  
50  
51  
52  
53  
54  
55  
56  
57  
58  
59  
60

Tobin DJ, Hagen E, Botchkarev VA, Paus R (1998) Do hair bulb melanocytes undergo apoptosis during hair follicle regression (catagen)? *J Invest Dermatol* 111:941-947.

Tobin DJ, Slominski A, Botchkarev V, Paus R (1999) The fate of hair follicle melanocytes during the hair growth cycle. *J Invest Dermatol Symp Proc* 4:323-332.

Toth BI, Benko S, Szollosi AG, Kovacs L, Rajnavolgyi E, Biro T (2009) Transient receptor potential vanilloid-1 signaling inhibits differentiation and activation of human dendritic cells. *FEBS Lett* 583:1619-1624.

For Review Only